MASTERARBEIT | MASTER'S THESIS

Titel | Title

Colitis-associated CRC in young vs. old mice

verfasst von | submitted by

Gitta Frisch BSc

angestrebter akademischer Grad | in partial fulfilment of the requirements for the degree of

Master of Science (MSc)

Wien | Vienna, 2024

Studienkennzahl lt. Studienblatt | Degree programme code as it appears on the student record sheet:	UA 066 834
Studienrichtung lt. Studienblatt | Degree programme as it appears on the student record sheet:	Masterstudium Molekulare Biologie
Betreut von | Supervisor:	Assoz. Prof. Dr. Enikö Kallay

Table of contents

Acknowledgement

I would like to express my deepest gratitude to Prof. Univ.-Doz. Mag. Dr. Enikő Kállay for welcoming me into her research group again, and for trusting me with the given project while giving her advice and assistance. I would like to extend my great gratitude to Priv.-Doz. Mag. Dr. Martin Schepelmann for his patient guidance and valuable critiques during the planning and development of this thesis. His willingness to give his time so generously has been very much appreciated. I am very thankful for Valeriya Guschina and Karina Piatek for their supportive encouragement and good advice in laboratory techniques.

I would also like to thank Teresa Manhardt for her supervision and help with the IHC stainings. Finally, I would also like to thank Sarah Guttmann for their useful and constructive technical recommendations on spectrophotometric evaluations.

Abstract

Colorectal cancer ranks as the third most prevalent cancer worldwide and stands as the second leading cause of cancer-related deaths. Despite being primarily a disease of the elderly, the majority of the animal models are on young mice, typically around 3 months old. To enhance our comprehension of colitis-associated colorectal cancer, I am working with aged mice (18 months) from the Balb/C and C57Bl/6 mouse strains. By doing so, I hope to narrow the disparity between experimental models and the intended target population. My objective is to investigate the impact of anti-inflammatory treatment with mesalazine on the emergence of colon cancer in both young and old mice. In pursuit of this goal, I am comparing how colitis-associated cancer induction occurs in mice, considering factors such as age, strain, and treatment approach.

The methodical part of the work started by isolating RNA from the colonic tissue of mice subjected to AOM/DSS treatment, a protocol known to promote the development of colon cancer. Throughout the steps of RNA extraction, RT-qPCR analysis, and immunostainings, I was able to assess how aged mice respond to anti-inflammatory treatment with 5-ASA.

The results showed a distinctive treatment response that differs depending on age, genetic strain, and the specific segment of the colon under consideration. The ascending colons of the young Balb/C mice were the most sensitive to treatment, while the older mice exhibited minimal to no reaction to the treatment, irrespective of the strain. This outcome highlights how anti-inflammatory therapies can have different outcomes based on age, strain, and colonic segment of the mice used. It also sheds light on the importance of considering age-related variations in designing treatment strategies.

In summary, this study highlights the many-sided nature of the anti-inflammatory response trough the 5-ASA treatment, underlining how the old mice show little to no response to the treatment. The increased sensitivity observed in young Balb/C mice shows the significance of tailored therapeutic approaches by using optimized treatments that take into consideration how age-related treatments can be important based on the different reaction to the anti-inflammatory treatment.

Zusammenfassung

Darmkrebs ist weltweit die dritthäufigste Krebserkrankung und die zweithäufigste Ursache für krebsbedingte Todesfälle. Trotz der Tatsache, dass es sich hauptsächlich um eine Krankheit der älteren Menschen handelt, werden die meisten Tiermodelle an jungen Mäusen, typischerweise etwa 3 Monate alt, durchgeführt. Um unser Verständnis von kolitis-assoziiertem Darmkrebs zu verbessern, arbeite ich mit älteren Mäusen (18 Monate) der Balb/C und C57Bl/6-Mausstämme. Dadurch hoffe ich, die Diskrepanz zwischen experimentellen Modellen und der Zielpopulation zu verringern. Mein Ziel ist es, die Auswirkungen einer entzündungshemmenden Behandlung mit Mesalazin auf das Auftreten von Darmkrebs sowohl bei jungen als auch bei alten Mäusen zu untersuchen. Im Zuge dessen vergleiche ich, wie die Induktion von kolitis-assoziiertem Krebs bei Mäusen unter Berücksichtigung von Faktoren wie Alter, Stamm und Behandlungsansatz erfolgt.

Der methodische Teil der Arbeit begann mit der Isolierung von RNA aus dem Kolongewebe von Mäusen, die der AOM/DSS-Behandlung unterzogen wurden, einem Protokoll, das die Entwicklung von Darmkrebs fördert. Durch die Schritte der RNA-Extraktion, RT-qPCR-Analyse und Immunfärbungen konnte ich beurteilen, wie ältere Mäuse auf die entzündungshemmende Behandlung mit 5-ASA reagieren.

Die Ergebnisse zeigten eine markante Behandlungsreaktion, die je nach genetischem Stamm spezifischen Segment des Kolons und Alter unterschiedlich war. Die aufsteigenden Kolons der jungen Balb/C-Mäuse waren am empfindlichsten gegenüber der Behandlung, während die älteren Mäuse unabhängig vom Stamm eine minimale Reaktion auf die Behandlung zeigten. Dieses Ergebnis verdeutlicht, wie entzündungshemmende Therapien je nach Alter, Stamm und Kolonsegment der verwendeten Mäuse unterschiedliche Ergebnisse haben können. Es zeigt auch die Bedeutung der Berücksichtigung altersbedingter Unterschiede bei der Gestaltung von Behandlungsstrategien auf.

Zusammenfassend zeigt diese Studie die vielfältige Natur der entzündungshemmenden Reaktion durch die 5-ASA-Behandlung und unterstreicht, dass ältere Mäuse wenig bis gar nicht auf die Behandlung ansprechen. Die erhöhte Empfindlichkeit, die bei jungen Balb/C-Mäusen beobachtet wurde, zeigt die Bedeutung maßgeschneiderter therapeutischer Ansätze, bei denen optimierte Behandlungen in Betracht gezogen werden, die altersbedingte Behandlungsunterschiede berücksichtigen.

Introduction

Colorectal Cancer

As of today, colorectal cancer (CRC) is the third most common cancer and the second leading cause of cancer related deaths worldwide. [1]

Colorectal tumors start within the colon or rectum as lesions on the mucosal lining, from which they have the capacity to proliferate outward, traversing various layers. The cancerous cells can intrude into blood vessels or lymph vessels, facilitating their travel to distant locations in the human body, a phenomenon known as metastasis. [2]

The stage of colorectal cancer, indicating the extent of its spread, depends on how deeply it penetrates the colon or rectal wall and whether it has advanced beyond these primary areas.[2] The classification system employed for colorectal cancer (CRC) is the tumor-node-metastasis (TNM) staging. The "T" denotes the degree of tumor invasion into different layers of the bowel wall. The "N" indicates the quantity of lymph nodes affected, while the "M" signifies the existence of distant metastasis. In colorectal cancer (CRC), the stages are defined as follows: Stage I represents cancer that is limited to the bowel wall and does not involve the nearby lymph nodes. Stage II indicates that the cancer has not spread to the lymph nodes. Stage III suggests that while the cancer has not metastasized to distant organs, it has affected nearby lymph nodes. Finally, Stage IV indicates that the cancer has spread to distant organs at the time of diagnosis. [3]

CRC and Age

There are many risk factors that contribute to the development of CRC, including age, sex, race/ethnicity, and family history. [4] Some risk factors are modifiable and can decrease the possibility of developing CRC. Such factors are obesity, diet, physical activity, giving up smoking, and reducing alcohol intake. Furthermore, a healthier diet that´s rich in leafy greens, dietary fiber and calcium have been reported to be protective against the development of CRC.[5]

Additionally, there are risk factors beyond one´s control which are nonmodifiable. Such risk factors are as a personal or familial history of colorectal polyps or CRC, a personal history of inflammatory bowel disease, and the presence of type 2 diabetes.[6]

Although CRC can emerge during early- to mid-adulthood, particularly in patients with certain inherited predispositions, the bulk of cases occur in those individuals who are categorized as the average risk group. Among this demographic, age stands out as the foremost risk factor.[5] The likelihood of developing CRC significantly rises above the age of 50. Approximately 90% of new cases and 94% of CRC-related fatalities occur in individuals aged 50 and older. [5,6]

The high risk category encompasses individuals who have a personal or familial history of CRC, adenomatous polyps, inflammatory bowel diseases (IBD), and hereditary CRC syndromes.[7]

Highlighting the importance of screening, CRC usually exhibits a slow growth pattern, and typically does not produce symptoms until the tumors reach a significant size, often several centimeters in diameter. At this stage, it can easily block the passage of stool, resulting in symptoms such as cramping, pain, or bleeding. The majority of colon tumors develop trough a multistep process, which typically entails a series of histological, morphological, and genetic changes that accumulate gradually over time. [8]

Lynch syndrome

Lynch syndrome is the most prevalent hereditary cancer syndrome. It is the leading hereditary contributor to CRC, and the only known hereditary factor associated with endometrial cancer. The oncogenic tendency of Lynch syndrome arises from a collection of mismatch repair proteins. Dysfunctional regulation of mismatch repair proteins results in abnormally high instability in specific genomic areas known as microsatellites. As time passes, the accumulation of mutations in microsatellites and other regions in the genome can disrupt the synthesis of important cellular proteins, ultimately triggering tumorigenesis.[9]

Pathways of CRC development

As colorectal tumors are heterogeneous at a genetic level, they arise trough several separate pathways. These pathways include chromosome instability (CIN), microsatellite instability

(MSI), and serrated neoplasia pathways. Each pathway provides some insight about their pathogenesis mechanisms, albeit with some overlap. In addition, entirely new pathways are continually being identified.[10]

CIN pathway

The chromosome instability (CIN) pathway, is characterized by chromosome changes that include somatic copy number alterations caused by aneuploidy, deletions, insertions, amplifications, or loss of heterozygosity. [11,12]

The mechanisms responsible for CIN are typically identified by defects in chromosomal segregation. These defects may facilitate the untimely separation of sister chromatids and cause telomere shortening. These changes can affect genomic reorganization, impaired DNA damage response mechanisms, and loss of heterozygosity in tumor suppressor genes.[10]

MSI pathway

Contrary to the CIN pathway, colorectal tumors can also emerge through hypermutable pathways. These pathways are distinguished by frequent mutations in somatic DNA base pairs.[10]

Generally, DNA mismatch repair mutations can lead to instability within microsatellite regions. DNA microsatellites are repetitive sequences of nucleotides that occur in tandem, consisting of mono-, di-nucleotide, or even higher-order nucleotide repeats. In these regions the errors usually tend to accumulate because the DNA polymerase has difficulty in efficiently navigating and binding to these repetitive genome sequences.[10]

Inability to accurately determine the appropriate number of bases to insert into these invariable regions or even slippages during the synthesis of a new DNA strand (which generates a temporary insertion deletion loop) can give rise to a frameshift mutation. These mutations lead to the production of nonfunctional proteins. In tumor cells that exhibit the MSI phenotype the cells fail to identify and repair mismatched DNA, allowing them to maintain and replicate their mutations and accumulate additional ones. [10,13]

Adenoma – Carcinoma Sequence and Alternative Serrated Neoplasia Pathways

Most colorectal tumors originate from pre-cancerous polyps, which can be broadly classified into traditional tubular adenomas or serrated polyps. The formation of adenomas happens when normal mechanisms that regulate DNA repair and cell proliferation are disrupted. Due to the continued loss of surface cells from the intestinal mucosa, a constant epithelial renewal is required. The proliferation takes place only at the crypt base. As the mutated cells progress towards the inner lining of the colonic lumen, the terminal differentiation and eventual cell death (apoptosis) are disrupted, which are leading to the formation of adenomas. With time, adenomatous polyps grow, and discrete adenomas form. Over time, adenomatous polyps increase in size and display increasingly abnormal features (dysplasia), and can eventually gain the ability to invade surrounding tissues.[10]

Thirty years ago, the adenoma-carcinoma sequence was the only known pathway of colorectal carcinoma. However, this pathway doesn't encompass all instances of colorectal carcinoma. As of today, the serrated pathway has gained recognition as an alternative pathway to colorectal carcinoma. [14] In this pathway, precursor lesions known as serrated polyps or serrated adenomas progress to cancer. These polyps have a serrated appearance under the microscope and include subtypes such as hyperplastic polyps, sessile serrated adenomas, and traditional serrated adenomas. The serrated pathway is believed to account for a significant proportion of sporadic colorectal cancers, particularly those that arise in the proximal colon[15] Notably, certain case studies have uncovered that lesions originating from the serrated pathway exhibit accelerated carcinogenesis. There are also reports indicating rapid transformation from sessile serrated lesions to invasive colorectal carcinoma occurring within a few months.[16,17]

CRC and Colitis

Inflammatory Bowel Diseases (IBD) encompass chronic inflammatory conditions affecting the gastrointestinal tract. The two major types of IBD are Crohn's disease (CD) and ulcerative colitis (UC). These conditions cause lifelong inflammation and significantly diminish the quality of life for those who are affected, imposing lifelong challenges on the patients.[18] [19] Current treatments primarily focus on addressing the inflammatory response itself, with particular attention to reducing the recruitment of inflammatory cells [20]

Although the disease pathogenesis is not fully understood, inflammatory bowel disease (IBD) is characterized by chronic inflammation of the gastrointestinal tract in genetically susceptible individuals, who are exposed to environmental risk factors. [21] Today it is well recognized that patients with IBD are at an increased risk of developing colorectal cancer (CRC), primarily as the result of chronic intestinal inflammation.[22]

Moreover, patients with IBD have also been shown to be at increased risk of developing extra-intestinal malignancies, which is thought to be a consequence of immunosuppressive therapies and an underlying inflammatory state.[23]

As the population of patients with IBD grows and ages, there is also an inevitable increase in the risk of cancer development. Moreover, many of these patients may require cancer treatment, including chemotherapy, radiation, and immunotherapy, and many may require further treatment for their IBD. Thus, it is necessary that anti-inflammatory treatments remain current and adaptable to individual patient needs. If existing therapies are ineffective, there is a need to develop new treatments to provide improved care to those who require it. It is essential to strive for treatment optimization because cancer treatment is not a one size fits all solution. It is also valuable to investigate, whether an older demographic responds differently to the established anti-inflammatory therapy for colitis-associated colorectal cancer (CAC). If not, it may be necessary to implement new modifications and enhancements to better address each patient´s unique needs.

AOM/DSS model

The AOM/DSS model is a well-established model to induce colitis-associated CRC. The model utilizes chemical induction of DNA damage followed by repeated cycles of colitis.[24]

Azoxymethane (AOM)/ Dextran Sulfate Sodium (DSS) is introduced to the mice´s system (AOM is injected intraperitoneally, DSS was given into their drinking water) in order for them to develop colitis-associated colorectal cancer by the induction of DNA damage followed by repeated cycles of colitis. [25,26].

AOM is a procarcinogen that is taken up by the colonic epithelium after injection to the mouse. It´s procarcinogen effect is facilitated by G->A transitions in the DNA, and leads to mutations.[27] DSS is a polysaccharide that dissolves in the drinking water of the mice and inflicts colonic inflammation, marked by changes like the loss of crypt architecture, disruption of cellular junctions and ulcerations in the mucosal lining.[28] The damage to the cells lining of the colon prompts an influx of immune cells, to mediate both anti-pathogenic and anti-inflammatory functions which are helping the tissue repair and cell survival. [29,30]

Combining AOM and DSS provides a two-step tumor model for colitis-associated colorectal cancer (CAC). [31] Utilizing the AOM/DSS treatment has the advantage of assessing CRC triggered by occasional mutations caused by AOM, while also causing an inflammatory reaction (whose intensity varies based on the dosage of DSS administered).[32]

Mesalazine

The figure below (Figure 1) depicts mesalazine (or 5-ASA (5-aminosalicylic acid)), an anti-inflammatory drug used to treat IBD including UC and Crohn´s Disease. [33]

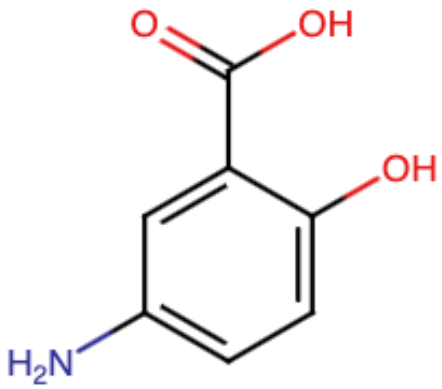

1. Figure:chemical structure of mesalazine (5-ASA). Image made by using chem-space.

The exact mechanisms of action are still unclear. It seems to work within the colon´s mucous membrane by reducing the inflammation trough a range of anti-inflammatory mechanisms.[33] However, other mechanisms of action of 5-ASA have been described, including the inhibition of mediators of lipoxygenase and cyclooxygenase, interleukin-1, interleukin-2, and tumor necrosis factor-alpha. 5-ASA has also been recognized to act as an antioxidant and free-radical scavenger.[34–36] 5-ASA is now believed to be involved in the control of cell proliferation,

apoptosis and metabolic functions besides the activation of a class of nuclear receptors involved in control of inflammation.[37]

Mouse strains

In the experimental setup, the two commonly employed inbred mouse strains, namely Balb/C (albino) and C57Bl/6 (black), were selected as research models. These strains are very favored in scientific research due to their well-established genetic stability, which arises from their homozygous nature.

Inbred strains are characterized by their formation through over 20 generations of breeding between siblings. [38] The individuals of an inbred strain are deemed indistinguishable, with any observed variations in traits primarily attributed to environmental differences. Because of this genetic uniformity, research can be conducted with relatively small sample sizes. Inbred strains are valuable for elucidating the genetic basis of characteristics such as susceptibility to infections or reactions to medications. This genetic uniformity of the mice ensures a consistent and well-defined phenotype within each strain, and also offers a reliable and unambiguous background information for the study.[39]

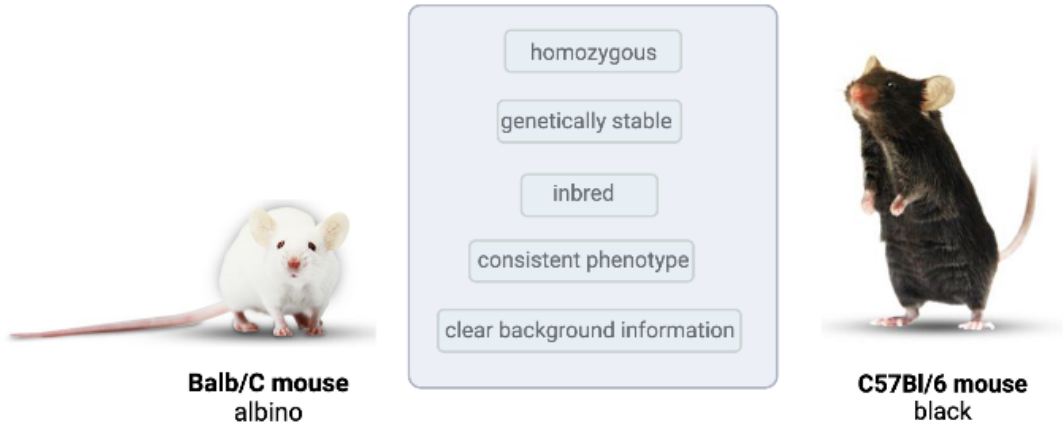

2. FigureThe mouse strains and their common characteristics that make them ideal for the conducted experiments. Created with BioRender.com, images used from cyagen.

While both Balb/C and C57/Bl6 strains (depicted above in Figure 2) share numerous similarities and are often assumed to have comparable characteristics, there are a few distinctions in their innate immune responses. These variations are due to differences in cytokine and leukocyte levels between the two strains, which implies that certain aspects of their immune systems may diverge. These differences in the innate immune responses could be of significance when interpreting experimental outcomes, and understanding potential differences in disease models or treatment responses.[40]

Ascending vs descending parts of the colon

The experimental protocol involved the collection of both the ascending and descending segments of the colons. As depicted in the figure below (in Figure 3), the ascending colon, positioned along the right side of the abdomen, primarily serves as a site for water absorption. However, the descending colon, which is in the lower abdomen, functions as a reservoir for fecal matter.

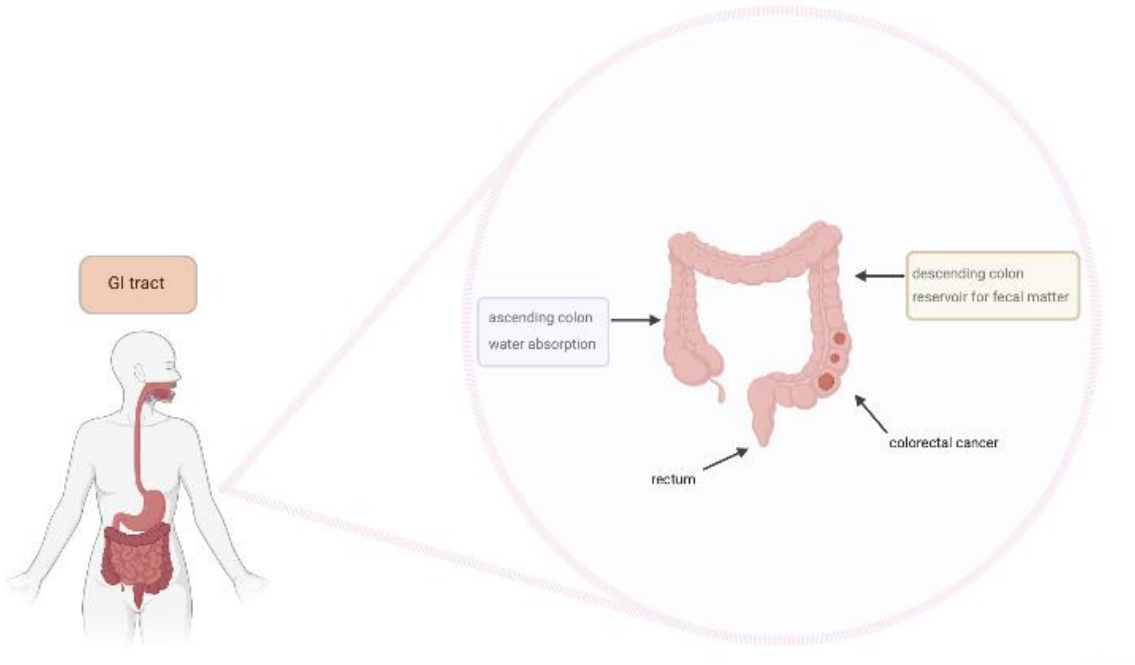

3. Figure: The ascending and descending parts of the colon. Figure created with BioRender.com.

It is important to mention that ascending and descending portions of the colon, depicted above in Figure 3, exhibit dissimilarities in terms of metabolite composition and epithelial morphology due to the differences of the mucus layer. [41] By evaluating both segments of the colon, a much more comprehensive assessment of the manifestations of these differences following AOM/DSS treatment can be made.

The colon spans around 150 cm in length, running from the ileocecal valve to the anus. It consists of seven segments: the cecum, ascending colon, transverse colon, descending colon, sigmoid colon, rectum, and anus. [42] The differentiation between right-sided and left-sided colon is rooted in their embryonic development. Specifically, the cecum, appendix, ascending colon, hepatic flexure, and the initial two-thirds of the transverse colon originate from the midgut. The remaining one-third of the transverse colon, splenic flexure, sigmoid colon, descending colon, and rectum originate from the hindgut. Tumors in right-sided colorectal cancer originate from the ascending colon and the proximal two-thirds of the transverse colon, while those in left-sided colorectal cancer develop from the descending and sigmoid colon, as well as the distal one-third of the transverse colon.[41,43]

CRCs that arise in the ascending or descending colon exhibit variations in age-specific and sex-specific incidence rates, as well as differences in clinical, pathological, and molecular characteristics of tumors.[44]

The variations in which how ascending and descending colon develop and function could reflect differing susceptibilities to the development of different types of cancer. Tumors in the ascending part of the colon appear to manifest a genetically more stable form of the disease and could possibly arise trough the same mechanisms that underlie hereditary nonpolyposis colon cancer. In contrast, tumors in the descending part of the colon show higher levels of genetic instability and may develop through the same mechanisms that underlie polyposis-associated CRC syndromes. Distal tumors show evidence of greater genetic instability and may develop in a way similar to CRC syndromes associated with the proliferation of multiple polyps.[45]

There are notable distinctions between the right and left sides of the colon, possibly causing tumors to evolve differently in these areas. For example, the ascending colon comes from the embryonic midgut and receives blood from the superior mesenteric artery. On the other hand, the descending colon develops from the hindgut, receiving blood from the inferior mesenteric artery while also being perfused by the superior mesenteric artery. Additionally, the distal colon also originates from the hindgut and is supplied by the inferior mesenteric artery. The capillary network around the ascending colon is multilayered, which may relate to its greater water absorption and electrolyte transport capacity. At the same time, the descending colon is single-layered.[46,47]

During the fetal development, the blood group antigens A, B, H and Le^b are expressed throughout the fetal colon, whereas in adulthood are exclusively found in the ascending colonic mucosa. Additionally, rectal mucosa produces acidic (sulphated or carboxylated) mucin, while the ascending colonic mucosa produces neutral mucin. Acidic mucin contributes to the protective function of the mucus layer in the colon by helping to lubricate the passage of stool, protect the colon lining from mechanical damage, and create a barrier against

harmful substances and pathogens. It is also suggested that sulfated mucins are involved in regulating cell division, however their production is reduced in adenocarcinomas.[48] [49,50]
The length of the crypts also vary between the ascending and descending colonic segments, the ascending colon features longer crypts on average than the descending colon[51]. Furthermore, the ascending colonic mucosa exhibits a lower apoptotic index, possibly due to reduced expression of the pro-apoptotic protein *Bak* compared to the descending colonic mucosa.[52]

Aim

In my thesis, I focused on age, as one of the main risk factors for developing CRC. Most animal models that are used for experiments for CRC research are conducted on young mice (3-month-old) even though it is a disease that affects the older population. To address this disparity and achieve a more comprehensive understanding of the disease, my investigation employed aged mice (18-months-old) to bridge the gap between the experimental model and the target population.

The aim of my research was to investigate how anti-inflammatory therapy with 5-ASA affects the development of colon cancer emergence in 18-month-old mice and to shed light on how the age influences the response to 5-ASA treatment.

Methods and materials

AOM/DSS Treatment

For the experiment the mouse strains C57BL/6 and Balb/C were used as they are two commonly used mouse strains in laboratory research. [53]

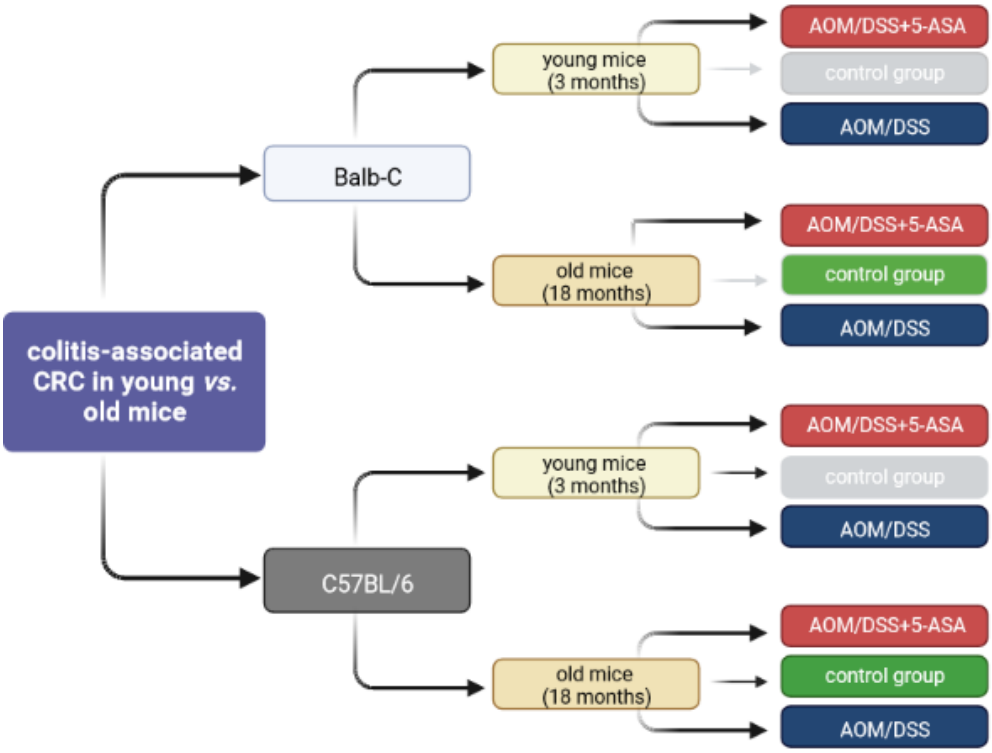

4. Figure: Overview of the mouse groups and the treatment they received. Figure was made with BioRender.com

The figure above gives an overview of the mouse strains that were used in the experiments, and the treatments they received. The results for the young mice were obtained by Nadja Kupper, a former PhD student of the Kallay group. I am using her results in order to better display the difference between how young *vs.* old mice react to 5-ASA treatment. The control groups for the young mice appear grey in the table above, as we did not have data from them at the end of my experiments.

For the experimental procedure (depicted in Figure 5), mice from two different strains at the age of 18 months were subjected to AOM/DSS treatment for a duration of 12 weeks. At the start of the first week, the mice were administered a single injection of 11.5 mg/kg AOM.

During the 2nd, 5th, and 8th weeks of the treatment, the mice were given 2.5% (w/v) DSS in their drinking water for 7 consecutive days. Following the completion of the 12-week treatment, the mice were euthanized, and their colons were collected for further analysis.

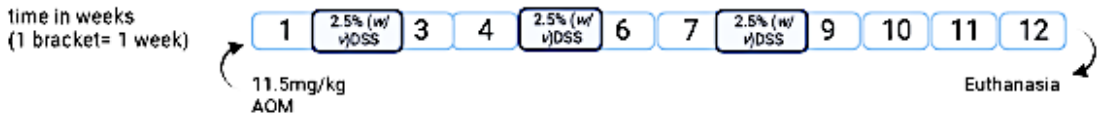

5. Figure: An overview of the AOM/DSS treatment. Figure was made with BioRender

RNA Isolation

After the colons were collected, the RNA was extracted from the colon tissues using the Promega ReliaPrep RNA Tissue Miniprep System. Initially, 500 µl of LBA+TG buffer was pipetted onto the colon tissues for lysis, and subsequently, the samples were placed in a tissue homogenizer.

An equal amount (500 µl) of RNA dilution buffer (RDB) was pipetted onto the samples following homogenization, and the samples were mixed by vortexing for 10 seconds. After vortexing, the samples were placed into a centrifuge for 10 minutes at 10.000 g, after which the lysates were removed and placed into new tubes, without debris.
340 µl isopropanol was added to the samples.

For the subsequent procedures, the minicolumns provided in the ReliaPrep kit were placed atop the collection tubes, and 700 µl of the lysates were carefully transferred into the minicolumns. The minicolumns were then subjected to centrifugation at 12,000–14,000 × g for 1 minute. Following centrifugation, the minicolumns were detached, and any remaining liquid in the collection tubes was discarded. Subsequently, the minicolumns were reinserted into the collection tubes, and the centrifugation step was repeated. After the two centrifugation steps, 500 µl of RNA Wash Solution was added to the minicolumns, centrifuged at 12,000–14,000 × *g* for 30 seconds and the liquid from the collection tubes was discarded again.

For the next incubation step a DNase 1 incubation mix was prepared by combining the following reagents:

24 µl of Yellow Core buffer

3 µl 0.09 M $MnCl_2$

3 µl of Dnase 1 enzyme

30 µl of the incubation mix was applied directly to the membrane inside the minicolumn.

The role of the DNase is to reduce viscosity and to remove the moderate amount of DNA contamination. After making sure that the membranes are completely covered by the incubation mix the samples were left to incubate on room temperature for 15 minutes, before 200 µl of the Column Wash Solution was added to the minicolumns and they were centrifuged at 12,000–14,000 × *g* for 15 seconds.

Following this step, the minicolumns were washed two more times, first time with 500 µl and the second time with 300 µl of RNA Wash Solution.

Following the two washing steps, the minicolumns were taken out from the collection tubes and transferred to 1.5ml elution tubes. To elute the RNA, 30 µl of nuclease-free water was added to the minicolumns. The tubes were then centrifuged at 12,000–14,000 × *g* for 1 minute. After centrifugation, the minicolumns were removed and discarded, leaving the isolated RNA from the samples in the elution tubes with the 30 µl of nuclease-free water.

Agarose gel electrophoresis was performed to check if the RNAs were still intact. The samples were run on a 1% agarose gel for 35 minutes at 100V. After the run was completed, the bands for the subunits of the RNA (28S, 18S and 5S) were all detectable on the gel. I expected to see the 28S rRNA, 18S rRNA and the 5S rRNA band on the gel to confirm that no RNA was lost during the isolation.

The concentration and purity of the RNA samples were assessed using a spectrophotometer in units of ng/µl. The spectrophotometric analysis also provided information about the purity of the samples and the pollution by phenol. Both values for the samples were in the ideal range (A260/280: 1,60 - 2,00 for protein purity and A260/230: > 2,00 for ethanol and phenol purity).

Quantitative reverse transcription polymerase chain reaction

The quantitative reverse transcription polymerase chain reaction is widely used to identify DNA. Reverse transcription, the conversion of RNA to complementary DNA (cDNA), is the first step to measure gene expression. Thus, following the extraction and purification, the RNA was reverse transcribed using the High-Capacity cDNA Reverse Transcription kit (Applied Biosystems, USA) following the manufacturer's instructions.

Reverse transcription

Reverse transcription is the enzyme-mediated synthesis of a cDNA molecule from an RNA template.

1. Table: The components used for reverse transcription.

	1 sample	Unit
RT buffer	2	µl
dNTPs	0.8	µl
random primers	2	µl
reverse transcriptase	1	µl
RNase free H2O	4.2	µl
Total	10	µl

All components, depicted in the table above (3. Table), were maintained on ice. RNA and RNAse free water were added to each tube accordingly to have 1000 ng of RNA in every tube. After the finished reverse transcription, the cDNA was diluted 1:10 in new 8-strip PCR tubes with individual shielded caps (0.2 ml). After dilution, the additional component (primers, dNTPs and lastly the enzyme reverse transcriptase) were added to the tubes. After every component was mixed the samples were incubated according to the thermocycler protocol below.

Thermocycler set up

Primer annealing: 25°C for ten minutes

DNA polymerization: 37°C for 120 minutes

Enzyme deactivation: 85°C for five minutes

Hold: 4°C

Quantitative RT-PCR

RT-qPCR was performed with Power SYBR Green PCR master mix (Applied Biosystems) using a StepOne Plus Real-Time PCR device.

SybrGreen is a fluorescent dye that specifically attaches to double-stranded DNA. As the PCR progresses, increasing amounts of SybrGreen bind to the newly synthesized double-stranded DNA. This leads to a rise in the fluorescence signal, which can be observed in real-time. By plotting the fluorescence against the temperature to create a melting curve, the PCR product can be analyzed to determine target specificity and to check for the presence of a single PCR product. For each target, a master mix (Power SybrGreen PCR Master Mix (MM) from Applied Biosystems) containing specific primers for amplification of the target gene was prepared.

The housekeeping genes were measured in triplicates, while all the other targets and the negative control were run as duplicates. To normalize the gene expression of the targets and to account for small variations in for example cDNA concentration, the housekeeping genes Eef1b2 (eukaryotic translation elongation factor 1 β 2) and β-actin were used. The calibrator was used to normalize the expression of the targets between individual qPCR runs.

2. Table: Components of the quantitative RT-PCR

Components	**Volume in µL**
MM	6.5
Primer (5 µM stock)	0.5
water	4
sum	11
cDNA (1:10)	2
total	13

The components of the master mix were prepared according to the table above. First the 11µL of the MM was pipetted in every used well of the qPCR plate (MicroAmp Fast Optical 96-well Reaction Plate with Barcode 0.1 ml from Applied Biosystems, Thermo Fischer Scientific). In the subsequent stage, 2 µL of cDNA, which had been diluted 1:10 with water was added into each well of the plate. To ensure proper mixing of the contents, the plate was then sealed with optical adhesive film and centrifuged at 4 °C for 5 minutes at 1,000 x *g*.

After the PCR run was complete, the Ct value was then defined as the number of cycles it takes for each sample to pass a fixed fluorescence threshold. Samples with higher original mRNA content, and thus cDNA content after reverse transcription, reach this threshold quicker than the samples with originally fewer mRNA copies. The target Ct values are then normalized to the Ct values for the mean values of the two housekeeping genes β-actin and Eef1b2 of the same sample.

Analysis

For the analysis of the RT-qPCR results, the baseline was set between 3 and 12 and the threshold for Ct determination at 0.4. That way the amplification curve of all products was still linear. Afterwards the mean and the standard deviation of the duplicates was calculated to find potential outliers, which are more than 2 standard deviations to either side of the mean. The ΔCt value was calculated as follows: the Ct-mean of the mean of the housekeeping genes was subtracted from the Ct-mean of the target gene.

Housekeeping genes maintain basic cellular functions of the organism and their expression does not change under normal conditions, thus serving as internal reference genes in qPCR. That way they can be used as a reference to normalize the differences in the concentration of each target. [54] The ΔΔCt value was then calculated based on the ΔCt values. This was done by subtracting the ΔCt of the calibrator from the ΔCt of the target that was normalized to the calibrator. The calibrator serves as a standard for the expression of the targets.

The ΔΔCt value provides information about the change in target gene expression relative to the calibrator. The corresponding fold-change value is calculated using the formula: 2^(-ΔΔCt). It gives information about how much more or less mRNA is in a sample compared to the calibrator. After real-time PCR, the data analysis was done using Microsoft Excel to sort the data, and the graphs were drawn by GraphPad Prism version 9 (GraphPad Software Inc., San Diego, USA).

Immunohistochemical (IHC) stainings

Immunohistochemistry (IHC) is a technique that uses specific antibodies to locate and identify antigens in cells and tissues.[55]

The essential steps of Immunohistochemistry (IHC) can be outlined as follows: first, antigen retrieval is performed; then, the primary antibody is added; next, a secondary antibody is applied, which binds to the primary antibody. Finally, a detection reagent is introduced in order to precisely locate the primary antibody and to reveal the target antigen.[56]

Antigen retrieval entails pretreating the tissue sample to reverse the masking effect that is caused by fixation. This step allows for the unveiling of previously concealed antigens and making them more susceptible to antibody binding. By enhancing the accessibility of these antigens, antigen retrieval allows for more efficient and specific antibody-antigen interactions during the subsequent stages of the IHC procedure. This leads to a more accurate and more reliable detection and localization of target molecules within the tissues.[57]

The primary antibody, which may be either monoclonal or polyclonal[1], is carefully adjusted to achieve the ideal balance between staining the target tissue and reducing any unwanted background staining. To visualize the antigen-antibody interaction using light microscopy, either the primary or the secondary antibody is labeled. The secondary antibody specifically targets the immunoglobulin from the species, in which the primary antibody was made. The labeling allows for visualization and detection of the bound antibodies, which ensures the identification and localization of the target antigen within the sample.

In some cases, background staining can happen due to the nonspecific binding of antibodies. To minimize this, the samples are incubated with serum from the same species as the secondary antibody, or with a blocking agent.[55]

To ensure the accuracy of the staining process, negative controls are used to check for nonspecific binding of the secondary antibody. These controls involve treating the sample tissue in the same way as the experimental samples but leaving the primary antibody out.

By including these negative controls, I was able to verify the specificity of the staining and to differentiate between genuine antigen-antibody interactions and any background staining caused by nonspecific binding.[55]

Ki-67-staining:

1st antibody: KI67 570 Bioscience, (#41-5698-82, Thermo Fisher Scientific Inc., AT)

The steps of the KI67 staining were as follows:

1. Paraffin melting: I put the samples in oven for 25 minutes at 60°C.
2. Rehydration: I washed the samples with xylene (3x10 minutes) and then with ethanol. For the ethanol, each washing step took 5 minutes, the concentration of ethanol decreasing after each wash. (100% -> 30%). As the last rehydration step, I washed the samples with PBS (5 minutes).

[1] monoclonal antibodies are produced from a cell lineage by cloning a white blood cell and they can only bind the same epitope, whereas polyclonal antibodies are made of multiple cell lineages and bind to multiple epitopes.

3. Antigen retrieval: I preheated the citrate buffer (10mM, pH=6) up to boiling temperature in the steamer and let he slides boil for 20 min the hot buffer. After letting it cool for 20 min at room temperature, I washed them for 2x5 min in PBS.
4. I marked the tissues with Dako Pen, making a circle around each tissue on the slides.
5. Permeabilization: I put the slides into PBS-0.2% Tween for 5 minutes.
6. Blocking: For unspecific background blocking, to reduce the background due the antibodies already present in the tissue, I incubated the samples with 5% goat serum in PBS-0.2% Tween for 30 minutes at room temperature.
7. 1st antibody: I diluted KI-67-570 1:250 in 0.1% BSA in PBS and left it overnight in the humidifier chamber at 4°C.
8. Washing with PBS-0.05% Tween 3x5 minutes.
9. I diluted 4',6-diamidino-2-phenylindole[2] (DAPI) 1:1000 in PBS and applied 2-3 drops to the slides, which I then left for 15 minutes in the dark.
10. Washing 3 times in PBS-0.05% Tween for 5 minutes.
11. I rinsed the slides in double distilled water and mounted them with Fluoromount (Fluoromount-G™ Mounting Medium, Thermo Fisher Scientific).

After these steps the samples were stored on 4° C.

CD20-staining:

1st antibody: CD20 Abcam 64088

2nd antibody: AB FL647 goat-anti-rabbit

The steps of CD20 staining are as follows:

Stept 1. to 3. were identical to the first staining protocol.

4. Permeabilization & blocking: For unspecific background blocking, I incubated the samples with 5% goat serum in PBS-0.05% Tween for 60 min at room temperature.
5. 1st antibody: I diluted CD20 1:200 in blocking buffer and left it overnight in the humidifier chamber at 4°C.

[2] blue-emitting fluorescent compound used for staining nuclei

6. I washed the samples with PBS-0.05% Tween for 3x5 minutes.
7. 2nd antibody: I diluted AB FL647 goat-anti-rabbit 1:1000 in blocking buffer. I spun the secondary antibody down at 14.000 x *g* for 10 minutes at 4°C before applying 2-3 drops on each sample. Afterwards I incubated the slides for 1 hour at room temperature in the dark.

   I performed the steps 8. to 12. as in the protocol above.

The acquired data was analyzed with the software tools TissueQuest and TissueFAXS (TissueGnostics GmbH, Vienna, Austria). These tools help to quantify and analyse biomarkers within the colonic tissue samples by using digital image analysis techniques.

Results

RNA isolation and spectrophotometric evaluation

After RNA isolation, the samples were loaded onto an agarose gel (as seen in the 6. Figure) to see whether any of the samples have been lost during the extraction process and whether the RNA was intact. The isolation was successful, with all the samples showing the 28S rRNA, 18S rRNA and 5S rRNA bands. Since the samples were all intact, the actual experiments could be continued.

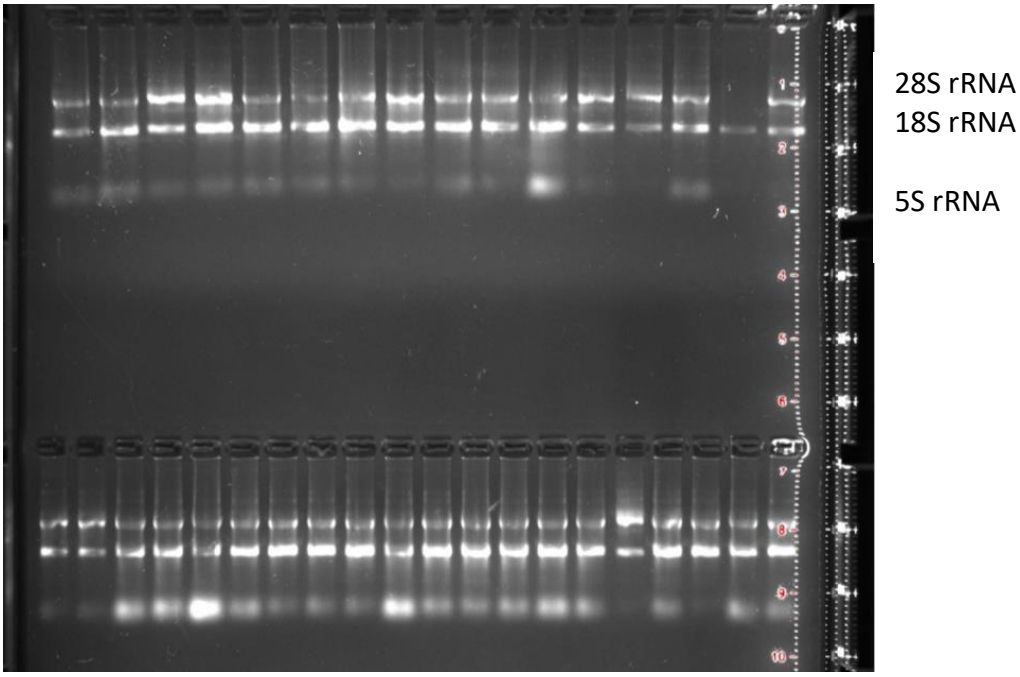

6. Figure: Representative gel electrophoresis of the intact samples from the descending colon. The subunits of the RNA are depicted on the right side of the figure next to the corresponding band. The 1% agarose gel was running on 100V for 40 minutes. The samples in the figure are of the descending parts of the colon

Expression levels of the targets

For reverse transcription PCR analysis, different targets were used to measure the effect of the 5-ASA treatment on the expression levels the targets in the 18-month-old mice from both strains. The housekeeping genes used were EEf1b2 and βactin, and the targets assessed were interleukine 6 (Il-6), cyclooxygenase 2 (COX-2), Bcl-2-associated X protein (BAX), B-cell lymphoma 2 protein (Bcl-2), Leucine-rich repeat-containing G-protein coupled receptor 5 (Lgr5), tumor necrosis factor alpha (Tnfα), Vitamin D3 24-hydroxylase (CYP24), 25-Hydroxyvitamin D 1-alpha-hydroxylase (CYP27), c-Myc, Calcium-sensing receptor (CaSR), Vitamin D receptor (VDR) and transcription factor 4 (Tcf4).

The targets were chosen to have a variety of inflammatory markers (such as IL-6, COX2 and Tnfα), as apoptotic markers (Bax and Bcl2) and markers of the vitamin D system (VDR, CaSR, CYP24A1 and CYP27B1) and the Wnt pathway (Lgr5 and Tcf4) to gain a comprehensive understanding of CAC development and its treatment across these areas.

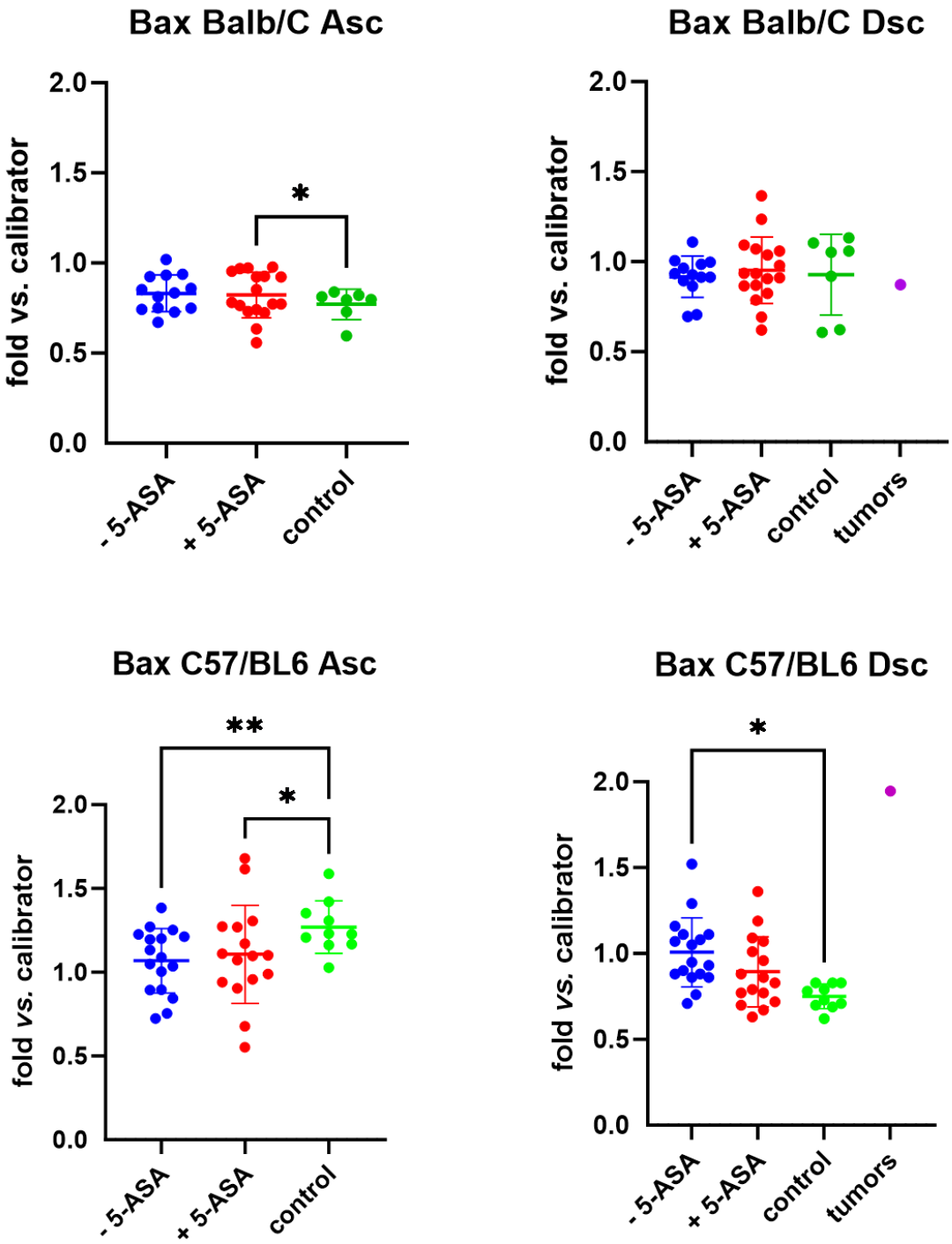

7. Figure: Figure: Expression levels for Bax in the ascending and descending colonic tissue of 18-month-old mice. The lines between the data points depict the mean expression levels while the values on the y-axis represent fold change expression vs. calibrator. Following a PCR, a two-way ANOVA (analysis of variance) was executed to evaluate the effects of multiple factors (strain and colonic segment) ont h results. Significantly distinct differences between groups are indicated by the presence of asterisks (P<0.05).

The figure above (Figure 7) presents a comparative analysis of Bax, a pro-apoptotic factor´s expression levels in the colonic tissue of 18-month-old Balb/C and C57Bl/6 mice in the ascending and descending colonic segments.

On the x-axis the mice in the various treatment groups are listed. The "-5-ASA" group refers to the group exclusively subjected to the AOM/DSS treatment without receiving any mesalazine. The "+5-ASA" category represents the group that received anti-inflammatory treatment with mesalazine after the AOM/DSS treatment. The "control" group, on the other hand, didn´t receive either the AOM/DSS treatment, or the mesalazine. During the mouse "sacrifice" two tumors were detected in the descending parts of the colonic tissues. One tumor was found in the desending colonic tissue of the Balb/C ice, the other tumor in the descending colonic tissue of the C57Bl/6 mice. Consequently, the decision was made to include them for descriptive but not statistical purposes, in order to enhance our understanding of how the anti-inflammatory therapy with 5-ASA affects the emergence of CRC emergence across all groups delineated on the x-axis.

In the Balb/C strain, the treatment with 5-ASA did not lead to any notable response in Bax expression levels. The expression levels of the pro-apoptotic factor Bax rose in the ascending colon upon receiving the AOM/DSS treatment compared to the control group, in the descending colonic segment.

In the C57Bl/6 mice, the AOM/DSS treatment led to a significant decrease in Bax levels compared to the control group in the ascending colon. Following anti-inflammatory treatment, the expression levels of Bax increased slightly, but didn´t get close to the levels of the control group, resulting in a significant difference between the two groups. Interestingly, the descending colonic tissue reacted differently, as the production of the pro-apoptotic factor Bax increased following AOM/DSS treatment, and only slightly decreased after anti-inflammatory treatment with 5-ASA.

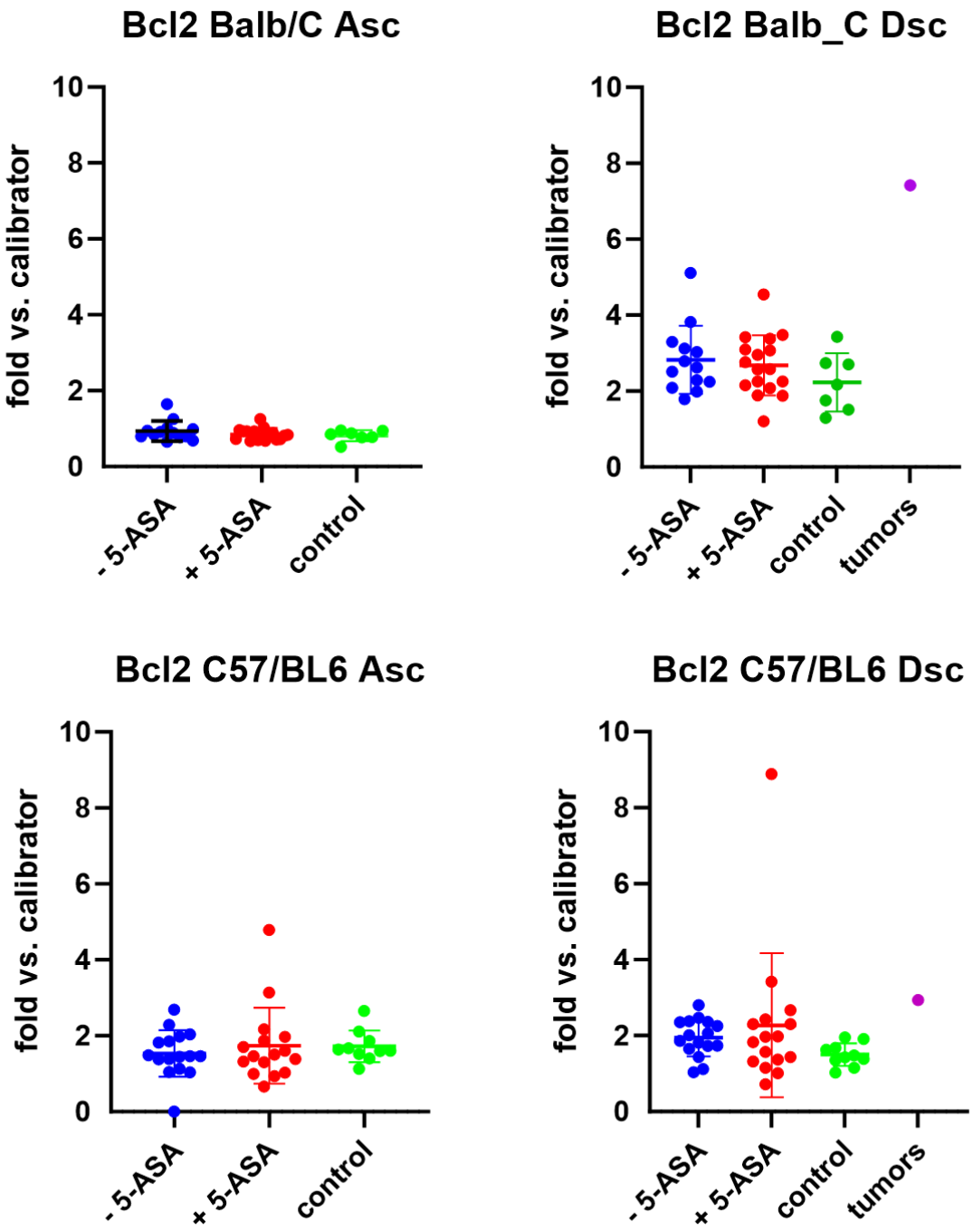

8. Figure:Expression levels for Bcl2 in the ascending and descending colonic tissue of 18-month-old mice. The lines between the data points depict the mean expression levels while the values on the y-axis represent fold change expression vs. calibrator. Following a PCR a two-way ANOVA (analysis of variance) was executed to evaluate the effects of multiple factors (strain and colonic segment) ont he results. Significantly distinct differences between groups are indicated by the presence of asterisks ($p<0.05$)

In the ascending colonic segment of the Balb/C mice, the expression levels of the anti-apoptotic factor Bcl2 remained similar among all groups, regardless of treatment (Figure 8.).

The AOM/DSS treatment and the administration of anti-inflammatory treatment with 5-ASA did not result in any notable change in Bcl2 expression levels.

Similar patterns were observed in the descending colonic tissues of the Balb/C mice. The Bcl2 levels stayed consistently low for each group. Similarly, the C57Bl/6 mice exhibited no change in their Bcl2 levels either. The expression rate remained consistently low in both the ascending and descending colonic segments, with no significant differences discernible between the groups. The anti-inflammatory treatment with mesalazine had no impact on the expression levels of Bcl2, as it remained unchanged in all groups that received this treatment. The tumor I the descending colon of the C57Bl/6 mice showed slightly higher expression level of Bcl2 compared to the other groups in this colonic segment.

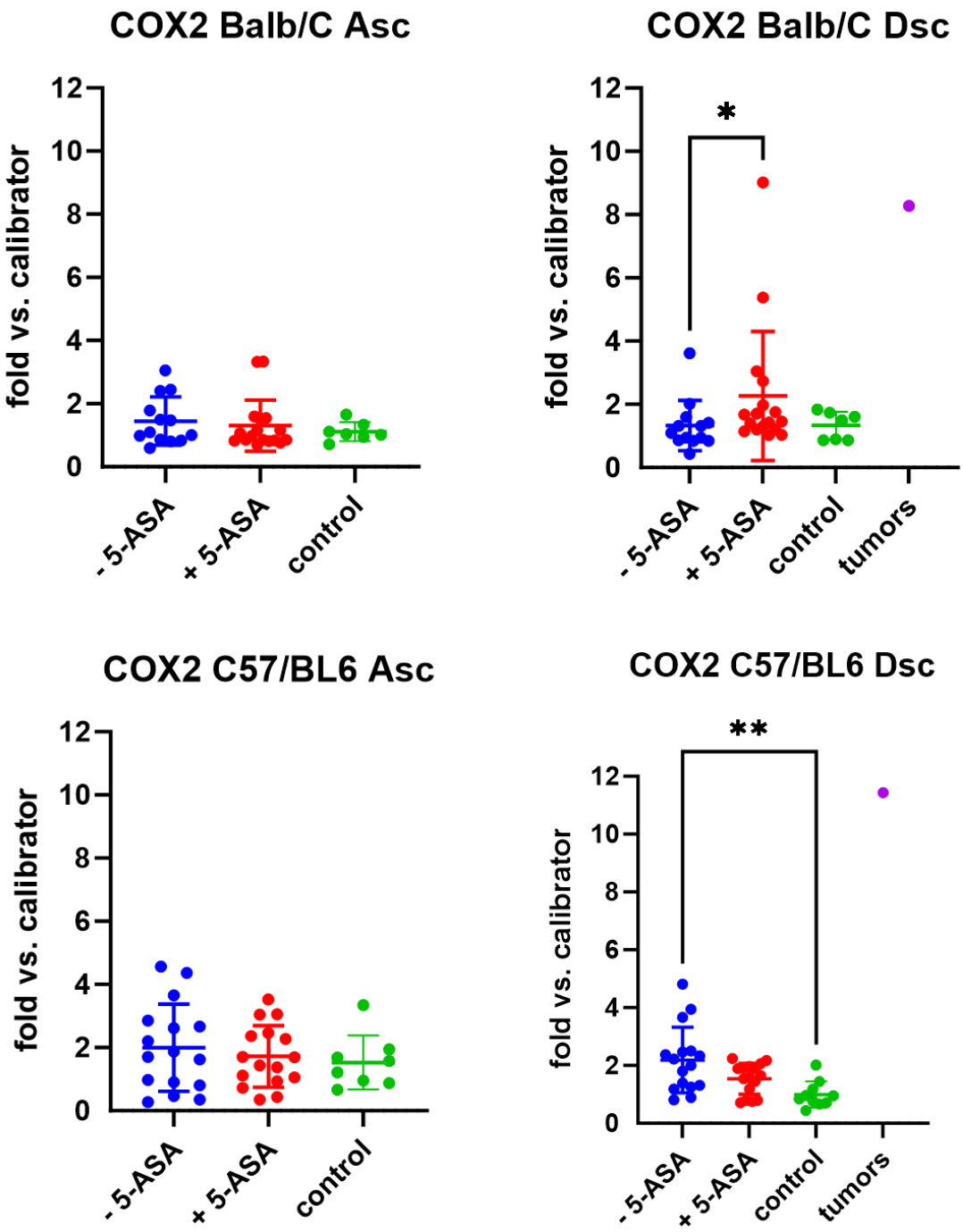

9. Figure: Expression levels for COX2 in the ascending and descending colonic tissue of 18-month-old mice. The lines between the data points depict the mean expression levels while the values on the y-axis represent fold change expression vs. calibrator. Following a PCR, a two-way ANOVA (analysis of variance) was executed to evaluate the effects of multiple factors (strain and colonic segment) on the results. Significantly distinct differences between groups are indicated by the presence of asterisks ($p<0.05$)

In the Balb/C strain, the administration of the AOM/DSS treatment led to an increase in the expression level, as seen compared to the control group. The introduction to mesalazine did not result in any changes in the expression levels of the pro-inflammatory marker COX2. Figure 9 also depicts that in descending colonic segments, all groups exhibited similar COX2 levels, independent of treatment.
In both descending colonic tissues of the mouse strains the tumor sample exhibited the highest COX2 expression levels.

In the ascending colon, the groups that received AOM/DSS treatment displayed slightly elevated COX2 expression levels compared to the ascending colonic tissues of the Balb/C mice. Mice that received anti-inflammatory treatment, and the control group, which didn´t receive any treatment, exhibited similar COX2 levels. In the descending colonic tissue of the C57Bl/6 mice, the tumor showed the highest COX2 levels. In this colonic segment, a significant difference emerged between the control group and the AOM/DSS treated group. The group that received the AOM/DSS treatment and subsequently developed CAC showed significantly higher expression rates of the pro-inflammatory marker COX2, compared with the control group.

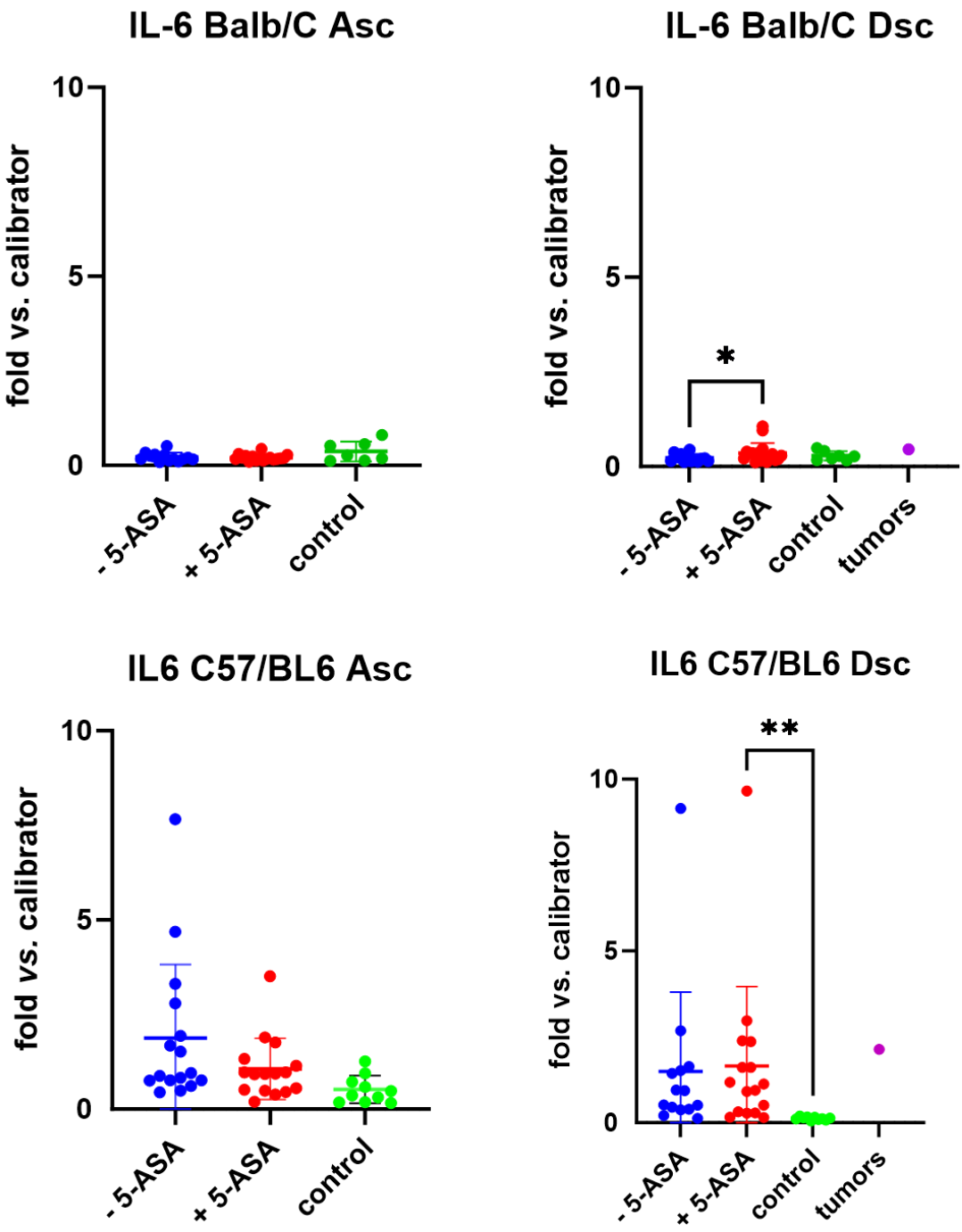

10. Figure: Figure: Expression levels for Il6 in the ascending and descending colonic tissue of 18-month-old mice. The lines between the data points depict the mean expression levels while the values on the y-axis represent fold change expression vs. calibrator. Following a PCR, a two-way ANOVA (analysis of variance) was executed to evaluate the effects of multiple factors (strain and colonic segment) on the results. Significantly distinct differences between groups are indicated by the presence of asterisks ($p<0.05$)

As seen in Figure 10, in the Balb/C mice, Il6 expression levels compared with the control group have similar expression levels as normal intestines. Both the ascending and descending colonic segment exhibited similar Il6 expression levels with no discernible difference between the groups. Following AOM/DSS treatment and subsequent anti-inflammatory intervention with 5-ASA, Il6 expression levels remained unaltered. Notably, neither the control group nor the tumor displayed any appreciable alteration in the expression levels of Il6.

In contrast, the C57Bl/6 mice exhibited a distinct response. In the ascending colon of C57Bl/6 mice, there was a subtle downregulation of Il6 following anti-inflammatory treatment, suggesting a reduction in colonic inflammation post-treatment. The control group within this strain displayed the lowest Il6 expression levels among all groups.

In the descending colon of the C57Bl/6 mice the Il6 levels decreased following the anti-inflammatory treatment, similarly to the trend observed in ascending colon, indicating strain specific regulation of the pro-inflammatory cytokine Il6. Notably, Il6 expression levels in the control group were similar with those of the group that underwent anti-inflammatory treatment, with the control group displaying the lowest Il6 levels compared with the experimental groups.

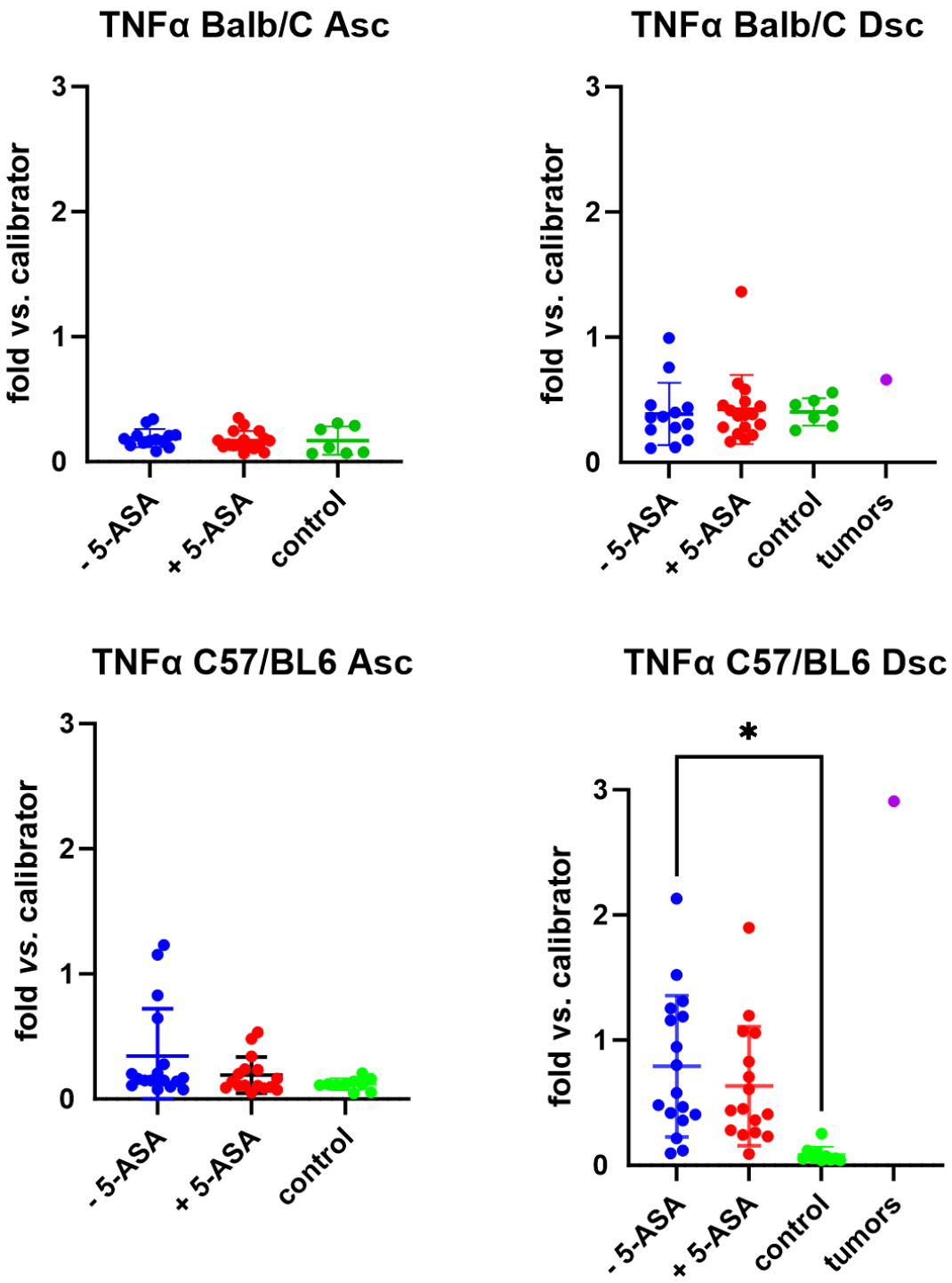

11. Figure: Expression levels for TNFα in the ascending and descending colonic tissue of 18-month-old mice. The lines between the data points depict the mean expression levels while the values on the y-axis represent fold change expression vs. calibrator. Followin a PCR, a two-way ANOVA (analysis of variance) was executed to evaluate the effects of multiple factors (strain and colonic segment) on the results. Significantly distinct differences between groups are indicated by the presence of asterisks ($p<0.05$)

In Figure 11 we can see that in the Balb/C strain the expression levels of TNFα in the ascending colonic tissue appeared to remain unaffected after the anti-inflammatory treatment with no observed change in expression levels among groups. While there was some more variation in the TNFα levels in the descending colonic tissue of the Balb/C strain, there was no significant difference between the groups. The control group also exhibited very low expression rates for TNFα, with no notable difference in the treated groups.

The C57Bl/6 strain showed higher expression levels of TNFα compared to the Balb/C strain. In the ascending colon of the C57Bl/6 mice the TNFα levels were slightly lower in the group that received anti-inflammatory treatment than in the AOM/DSS group. The tumor showed a drastically higher expression rate of TNFα than the other groups.
The descending colon of the C57Bl/6 mice, the TNFα levels were the highest overall, especially in the tumor, showing a stark contrast with the control group, which had the lowest TNFα levels in this colonic segment. The control group's expression was lower compared to the group without anti-inflammatory treatment.

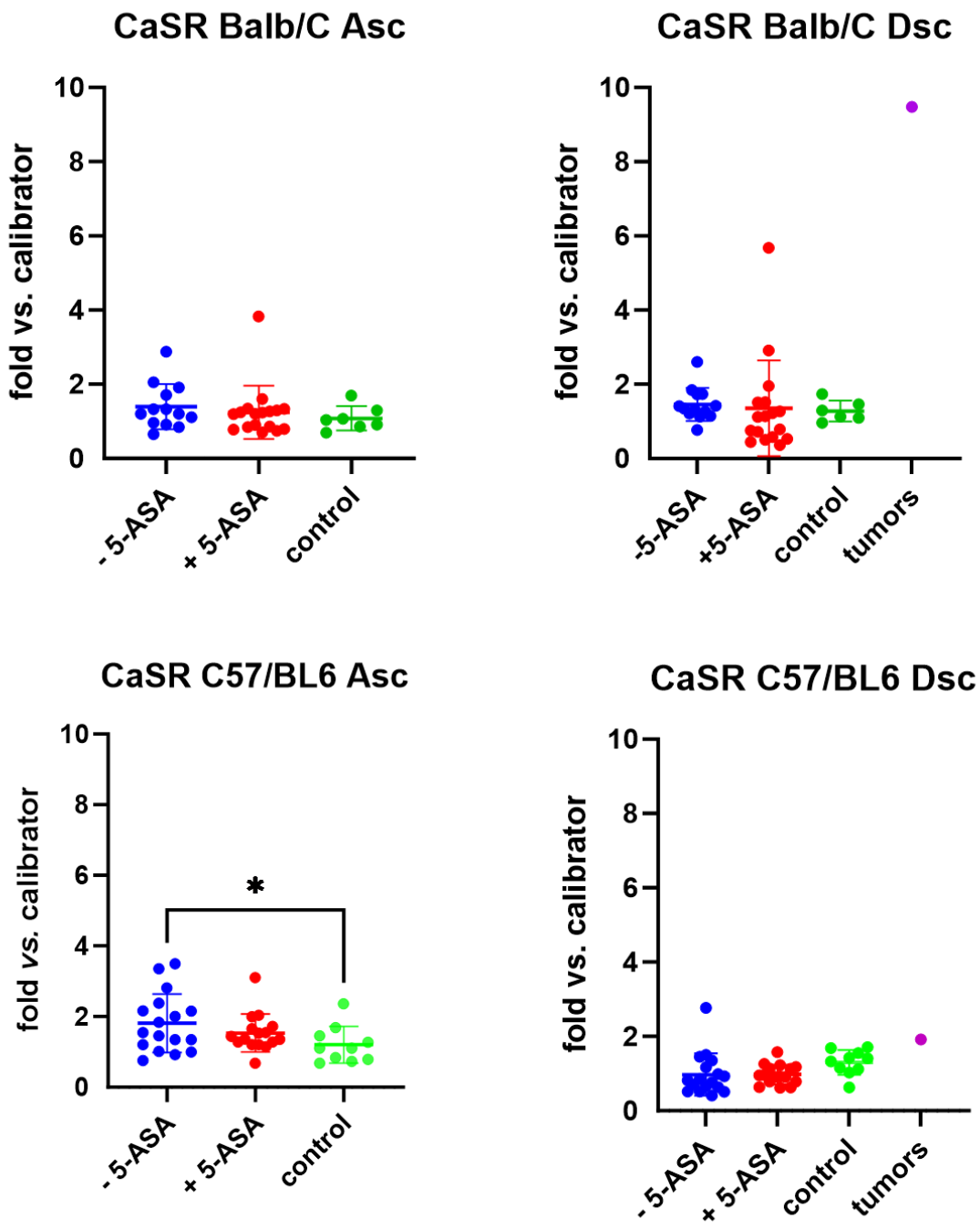

12. Figure: Expression levels for CaSR in the ascending and descending colonic tissue of 18-month-old mice. The lines between the data points depict the mean expression levels while the values on the y-axis represent fold change expression vs. calibrator. Followin a PCR, a two-way ANOVA (analysis of variance) was executed to evaluate the effects of multiple factors (strain and colonic segment) on the results. Significantly distinct differences between groups are indicated by the presence of asterisks ($p<0.05$)

Figure 12 depicts how after treating with the anti-inflammatory drug 5-ASA, the levels of CaSR were slightly reduced in the upper colon of Balb/C mice. However, there was no noticeable change in CaSR levels in the lower colon of these mice.

In C57Bl/6 mice, there were variations in CaSR expression levels between the ascending and descending colon tissues. In the ascending colon, the CaSR levels decreased upon receiving the anti-inflammatory treatment with mesalazine. The expression level was even lower in the control group. The tumor showcased an increase in CaSR expression levels.

Conversely, in the descending colon of C57Bl/6 mice, there was a subtle upregulation of CaSR levels following anti-inflammatory intervention. Notably, despite this modest increase, the control group consistently maintained elevated CaSR expression levels compared to the mesalazine-treated group.

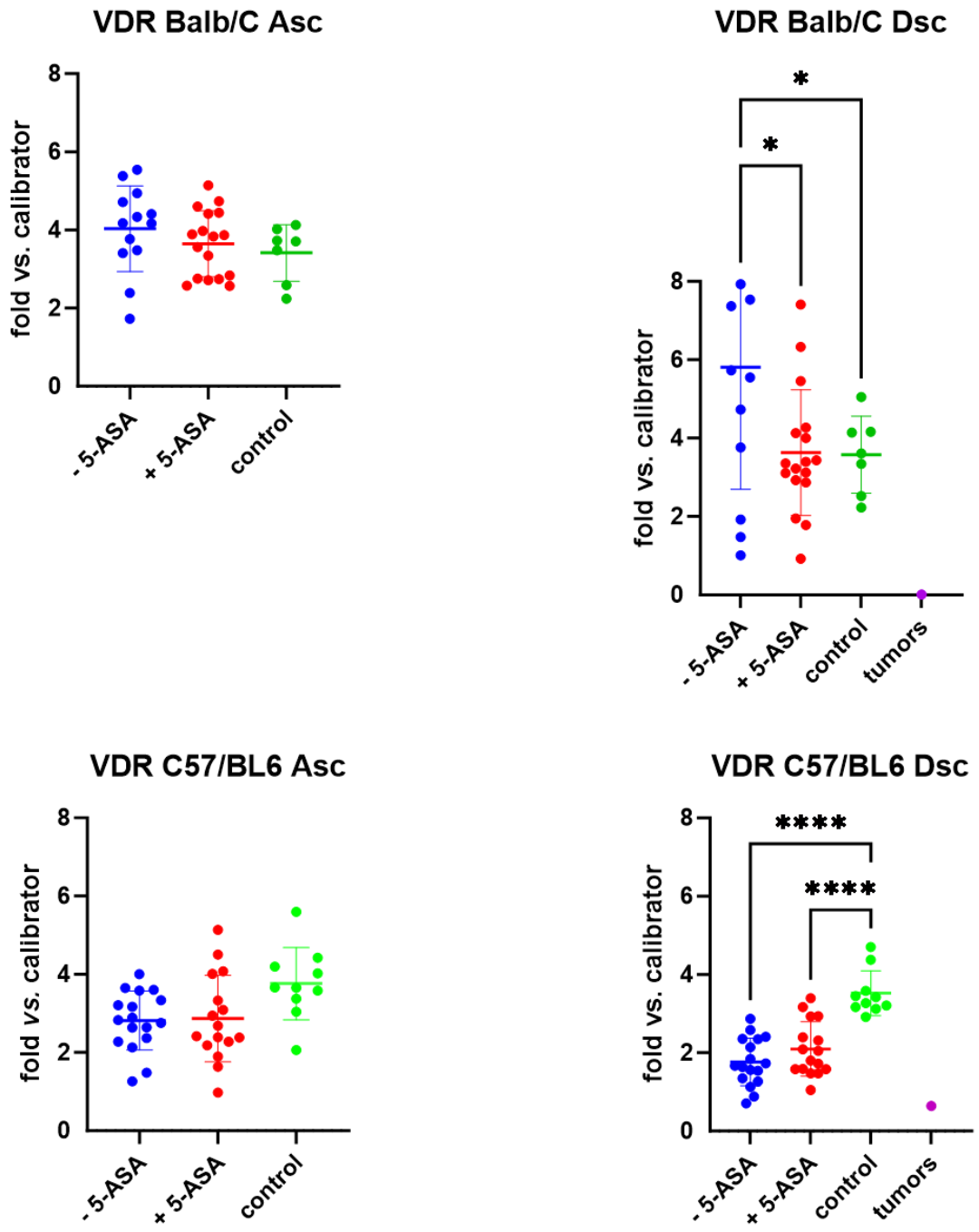

13. Figure: Expression levels for VDR in the ascending and descending colonic tissue of 18-month-old mice. The lines between the data points depict the mean expression levels while the values on the y-axis represent fold change expression vs. calibrator. Following a PCR, a two-way ANOVA (analysis of variance) was executed to evaluate the effects of multiple factors (strain and colonic segment) on the results. Significantly distinct differences between groups are indicated by the presence of asterisks ($p<0.05$)

In Balb/C mice, the administration of the anti-inflammatory agent 5-ASA resulted in a slight reduction of VDR expression in the ascending colon compared to the "-5-ASA" group that developed CAC. The control group exhibited even lower VDR expression, making the

AOM/DSS treated group the one with the highest VDR expression levels. Notably, the tumor had significantly lower VDR levels than the other groups, exhibiting the lowest VDR expression in the ascending colon.

In the descending colon of Balb/C mice, the "-5-ASA" group had even higher VDR expression levels than its counterpart in the ascending colon. The introduction of anti-inflammatory treatment led to a substantial decrease in VDR expression, particularly pronounced when compared to the changes observed in the ascending colon. The control group displayed markedly lower VDR levels compared to the group that did not receive 5-ASA treatment. It is noteworthy that, while the expression rates of VDR were similar between the control groups and the anti-inflammatory treatment groups, this was not the case for the group that did not receive 5-ASA treatment. In the descending colon, the tumor of Balb/C mice exhibited the lowest VDR expression, across both colonic segments and mouse strains, as depicted in Figure 13.

In the ascending colon of C57Bl/6 mice, an opposing response was observed with a slight increase in VDR levels upon introducing mesalazine. Notably, the control group exhibited the highest expression levels, establishing it as the group in this colonic segment of C57Bl/6 mice with the highest VDR levels, clearly surpassing those of the tumor.

Like the ascending colon, the descending colon of the C57Bl/6 strain displayed elevated VDR levels following anti-inflammatory treatment with 5-ASA. The disparity in VDR expression between the control group and the anti-inflammatory treatment group was substantial in this colonic segment, with the control group exhibiting significantly higher VDR expression than any other group. The difference was notably pronounced when compared to the -5-ASA group. Once again, the tumor exhibited the lowest VDR expression rates in both colonic segments and both strains.

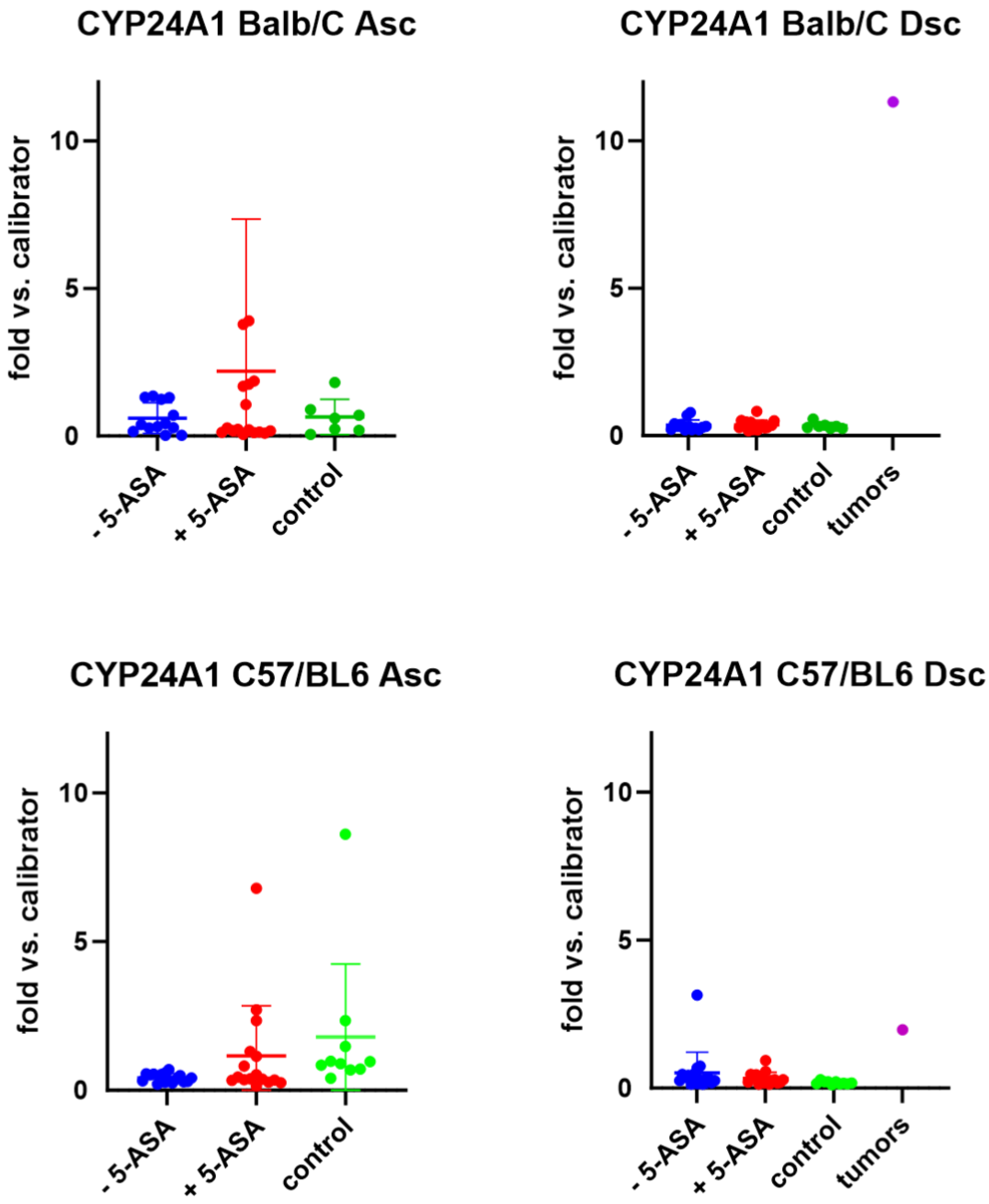

14. Figure: Expression levels for CYP24A1 in the ascending and descending colonic tissue of 18-month-old mice. The lines between the data points depict the mean expression levels while the values on the y-axis represent fold change expression vs. calibrator. Following a PCR, a two-way ANOVA (analysis of variance) was executed to evaluate the effects of multiple factors (strain and colonic segment) on the results. Significantly distinct differences between groups are indicated by the presence of asterisks ($p<0.05$)

As seen in Figure 14, in Balb/C mice, the administration of 5-ASA, an anti-inflammatory agent, resulted in an upregulation of CYP24A1 expression levels within the ascending colon. The CYP24A1 levels observed in the control group and the group without anti-inflammatory

treatment were nearly indistinguishable. Conversely, in the descending colonic tissue of Balb/C mice, the anti-inflammatory treatment demonstrated a lack of impact on CYP24A1 expression rates, with all experimental groups consistently displaying markedly low CYP24A1 levels, even lower than those observed in the ascending colon of Balb/C mice.

In contrast, in the ascending colon of C57Bl/6 mice, the anti-inflammatory treatment led to an increase in CYP24A1 expression levels. The control group within this colonic tissue exhibited higher levels of CYP24A1 expression compared to the ascending colon of Balb/C mice. Meanwhile, in the descending colon of C57Bl/6 mice, the expression levels of CYP24A1 were elevated in the tumors when compared to the other groups within the same colonic segment.

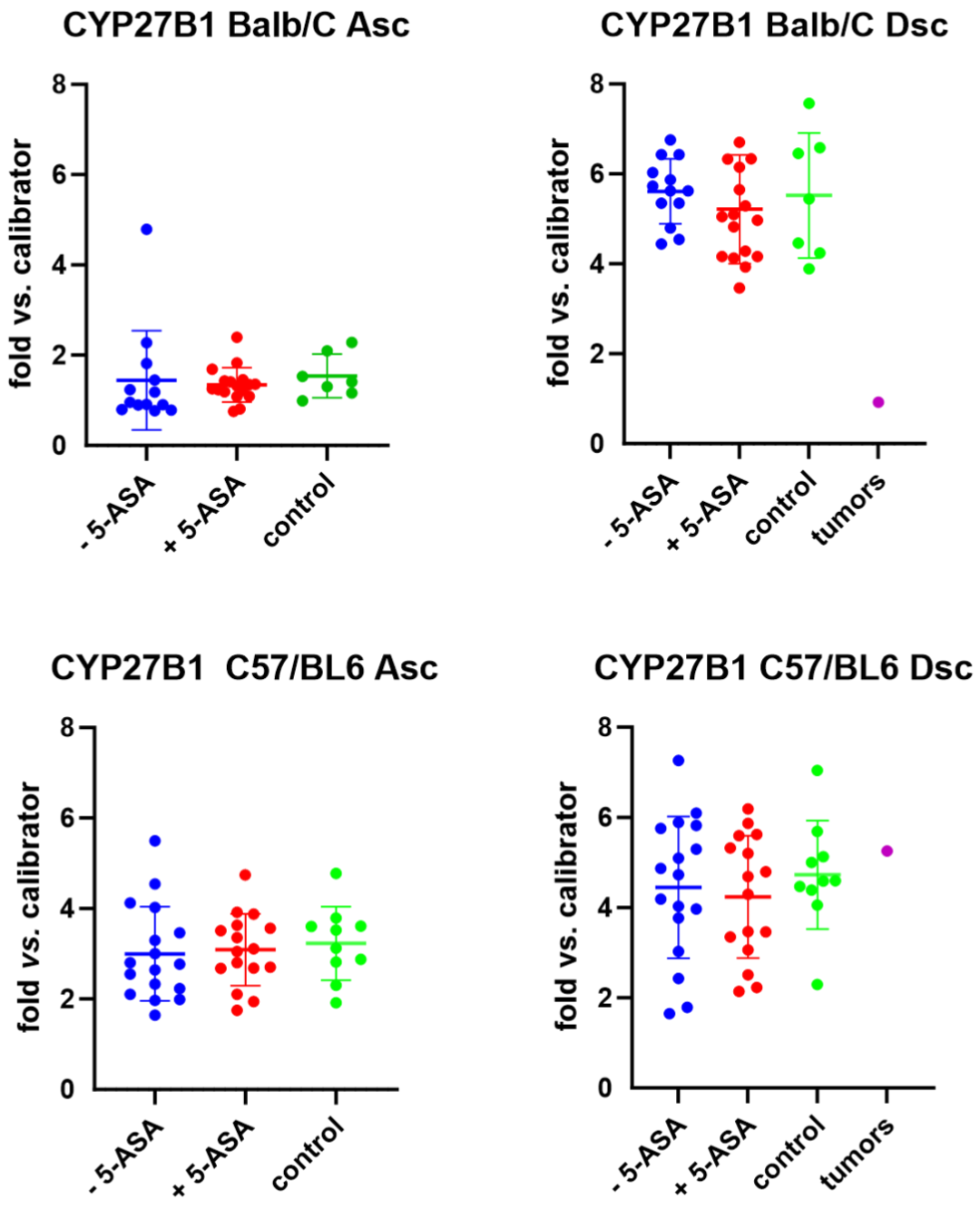

15. Figure: Expression levels for CYP27B1 in the ascending and descending colonic tissue of 18-month-old mice. The lines between the data points depict the mean expression levels while the values on the y-axis represent fold change expression vs. calibrator. Following a PCR, a two-way ANOVA (analysis of variance) was executed to evaluate the effects of multiple factors (strain and colonic segment) on the results. Significantly distinct differences between groups are indicated by the presence of asterisks ($p<0.05$)

In the ascending colonic tissue of the Balb/C mice the the anti-inflammatory treatment led to no notable impact on the expression level of CYP27B1. All group in this colonic segment

displayed consistently low expression rates for CYP27B1 than in the descending colon, as shown in Figure 15.

In contrast, the descending colon of the Balb/C mice showed higher expression levels than the ascending colon. Unlike in the ascending colon, the anti-inflammatory treatment led to a slight decrease in the CYP27B1 expression, making it slightly lower than the expression levels of the control group. Notably, the tumor in the descending colon displayed significantly lower CYP27B1 levels, about five times lower than the other groups.

In the ascending colon of C57Bl/6 mice, CYP27B1 levels were slightly elevated in comparison to those observed in Balb/C mice, yet no discernible alterations in CYP27B1 expression were detected in response to the anti-inflammatory treatment. However, in the C57Bl/6 strain, the tumor exhibited an upregulation of CYP27B1expression, approximately twice as high as the other groups. In the descending colon of the C57Bl/6 strain, akin to the descending colon of the Balb/C strains, the expression levels of CYP27B1 were elevated compared to the ascending colon, and like in the Balb/C strain, there was no significant difference in the expression rates between the groups.

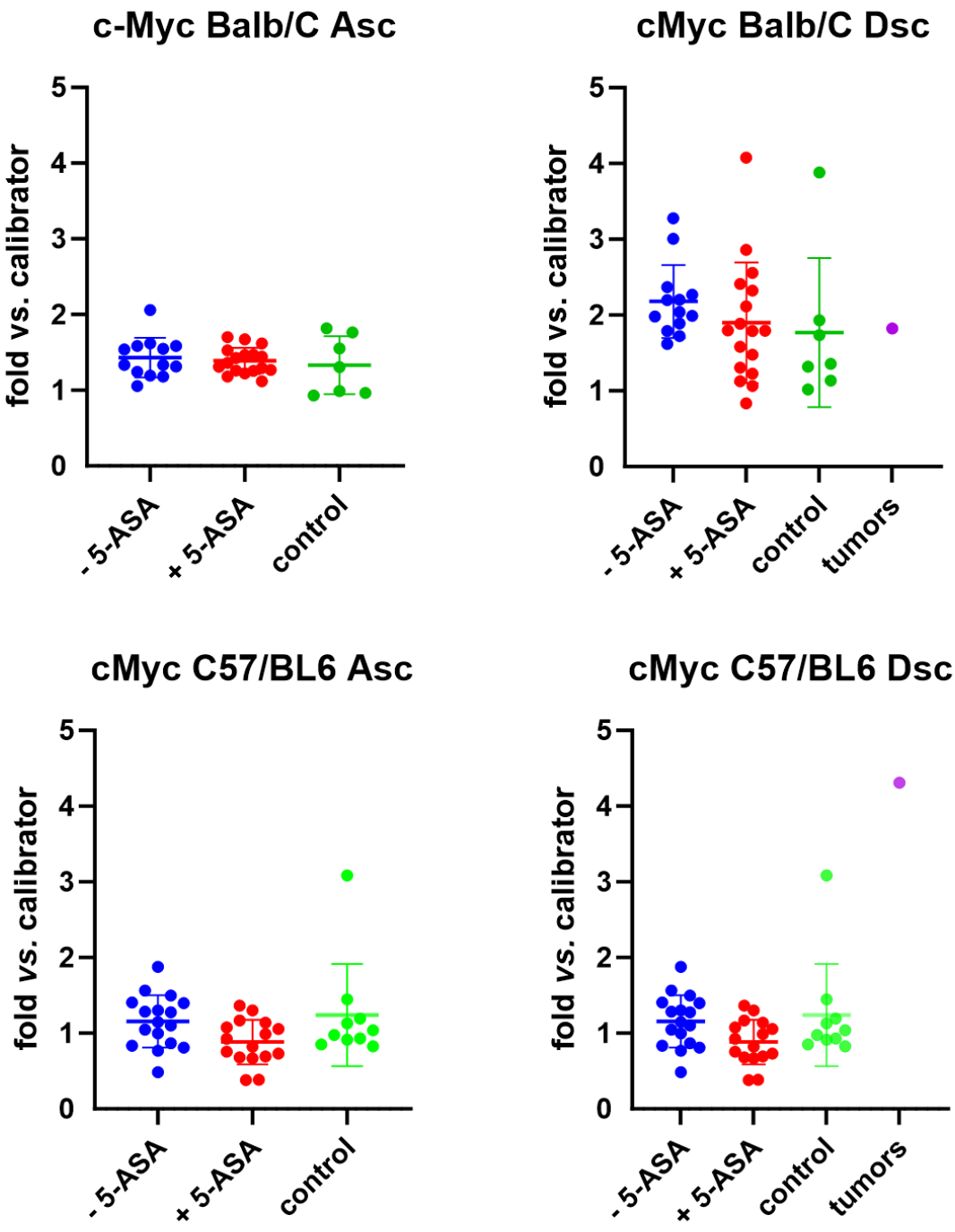

16. Figure: Expression levels for c-Myc in the ascending and descending colonic tissue of 18-month-old mice. The lines between the data points depict the mean expression levels while the values on the y-axis represent fold change expression vs. calibrator. Following a PCR, a two-way ANOVA (analysis of variance) was executed to evaluate the effects of multiple factors (strain and colonic segment) on the results. Significantly distinct differences between groups are indicated by the presence of asterisks ($p<0.05$)

In Balb/C strain mice, the administration of an anti-inflammatory treatment had minimal impact on the expression levels of c-Myc. In the ascending colon the c-Myc levels remained

similar across all groups, with similar expression levels to the calibrator, that are similar to healthy intestines, indicating normal expression levels independent of AOM/DSS or 5-ASA treatment. In the descending colon tissue of the Balb/C mice, the anti-inflammatory treatment with 5-ASA resulted in a slight decrease in the c-Myc levels. The control group and the tumor demonstrated comparable expression rates, mirroring the expression patterns observed in the ascending colon of Balb/C mice.

Figure 16 also depicts how In the C57Bl/6 mouse strain, the expression of the c-Myc gene was significantly elevated in tumors, showing a fourfold increase in comparison to other groups. In the ascending colon of C57Bl/6 mice, there was a slight reduction in c-Myc levels following anti-inflammatory treatment. The control group exhibited c-Myc levels like the group that received only AOM/DSS without anti-inflammatory treatment.

In the descending colon of C57Bl/6 mice, a similar increase in c-Myc expression was observed, mirroring what was seen in the ascending colon of these mice. Once again, the introduction of anti-inflammatory treatment with mesalazine resulted in a modest decrease in c-Myc expression levels, while the control group showed c-Myc levels similar to the group that did not receive anti-inflammatory treatment.

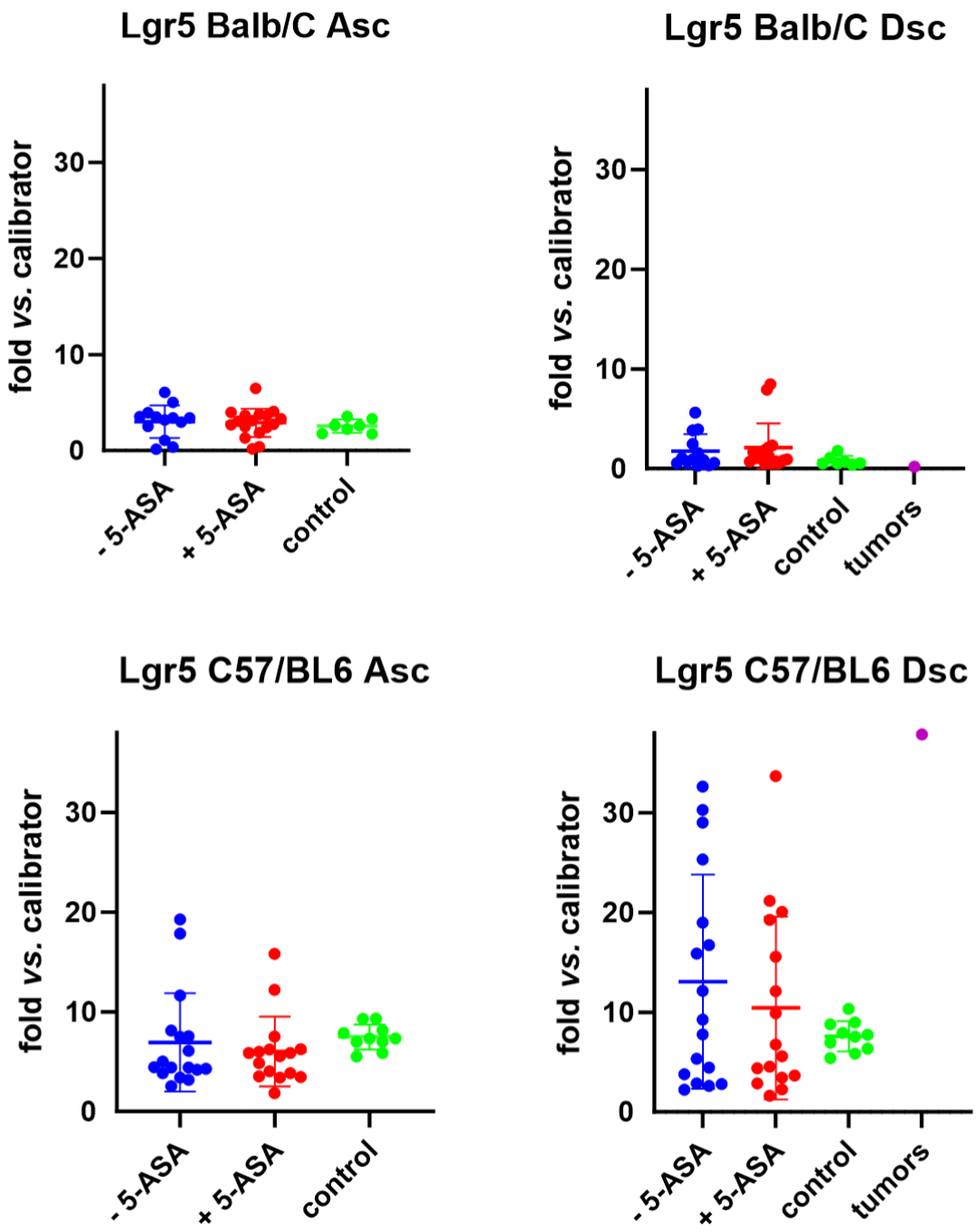

17. Figure: Expression levels for Lgr5 in the ascending and descending colonic tissue of 18-month-old mice. The lines between the data points depict the mean expression levels while the values on the y-axis represent fold change expression vs. calibrator. Followin a PCR, a two-way ANOVA (analysis of variance) was executed to evaluate the effects of multiple factors (strain and colonic segment) on the results. Significantly distinct differences between groups are indicated by the presence of asterisks ($p<0.05$)

In the Balb/C strain the Lgr5 expression levels didn´t exhibit any significant changes. Figure 17 demonstrates that while in the descending colon there was a slight increase in Lgr5 levels

following the anti-inflammatory treatment with 5-ASA, but in the ascending colon Lgr5 expression levels remained low.
However, a substantial increase in Lgr5 expression was observed in the tumor within the ascending colon. The expression rate of Lgr5 was approximately three times higher than in any other group within the ascending colon of the C57Bl/6 strain.

This upregulation of Lgr5 in the tumor was also to be observed in the descending colon of the C57Bl/6 mice.

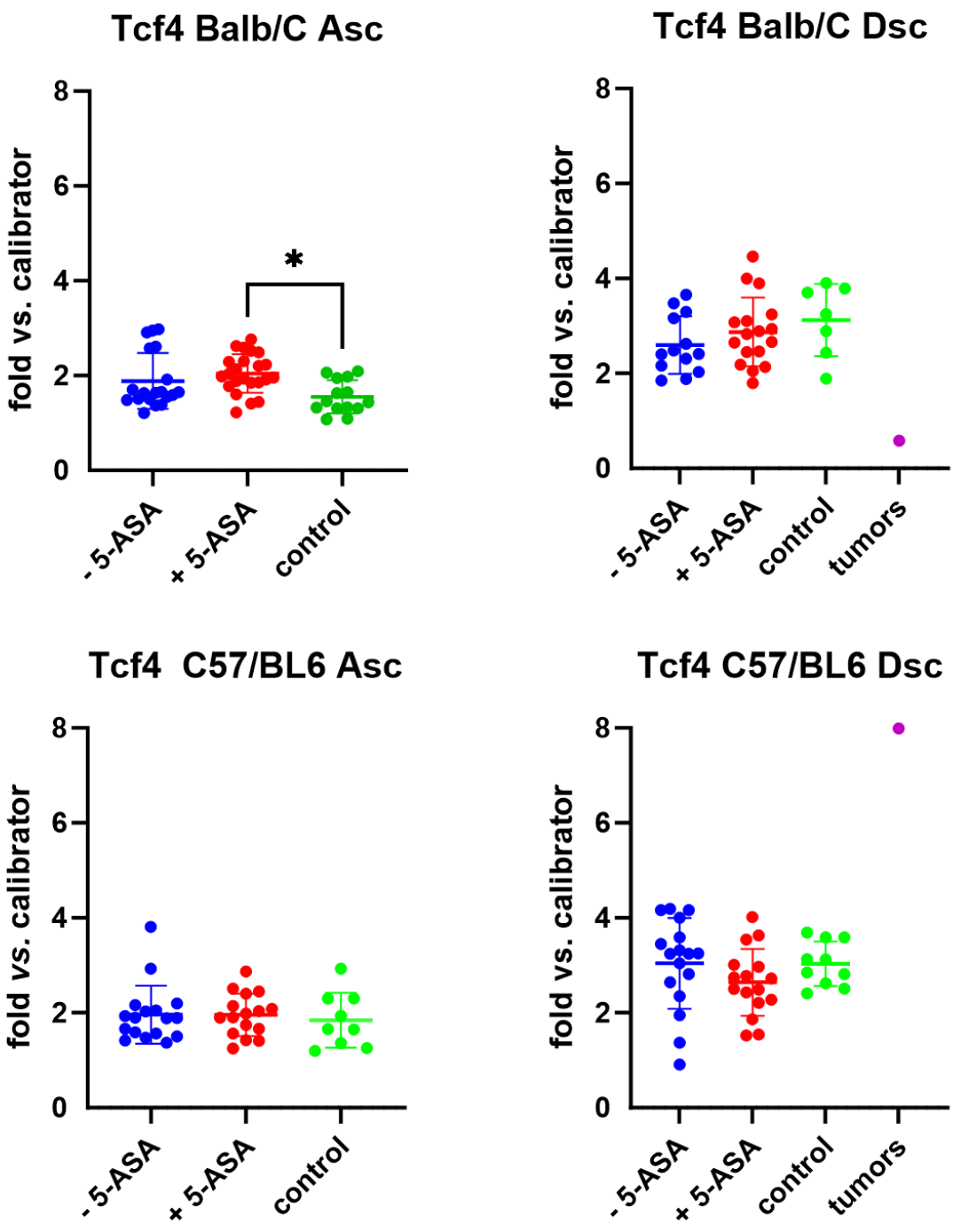

18. Figure: Expression levels for Tcf4 in the ascending and descending colonic tissue of 18-month-old mice. The lines between the data points depict the mean expression levels while the values on the y-axis represent fold change expression vs. calibrator. Following a PCR, a two-way ANOVA (analysis of variance) was executed to evaluate the effects of multiple factors (strain and colonic segment) on the results. Significantly distinct differences between groups are indicated by the presence of asterisks ($p<0.05$)

As depicted in Figure 18, in Balb/C mice, there was minimal variation in the gene expression levels of Tcf4, as the rates remained consistently similar across all groups. The only change in

Tcf4 expression was observed in the “+5-ASA” group that received mesalazine, as it was upregulated.

The anti-inflammatory treatment did not induce a substantial downregulation of Tcf4; however, the levels remained significantly higher than in the tumor. In the descending colonic tissue of Balb/C mice, the introduction of anti-inflammatory treatment led to a slight increase in Tcf4 expression levels. In this colonic tissue, the control group exhibited the highest Tcf4 expression levels, and the tumors, maintained the lowest expression rate for Tcf4 in the Balb/C strain.

Interestingly, the C57Bl/6 strain showed a different trend for Tcf4 expression. In this strain, the tumor appeared to have the highest Tcf4 expression, surpassing that of the other groups. In the ascending colonic tissue of C57Bl/6 mice, the introduction of anti-inflammatory treatment with 5-ASA did not alter Tcf4 expression; the levels remained consistently low, similar to the control group. This pattern was similar to the one observed in the descending colonic tissue of C57Bl/6 mice. Once again, the tumor displayed significantly elevated expression levels of Tcf4 compared to the other groups, and the anti-inflammatory treatment appeared to have no discernible effect on the mice, as their expression levels remained unaltered.

Effect of the treatment on proliferation and immune infiltration

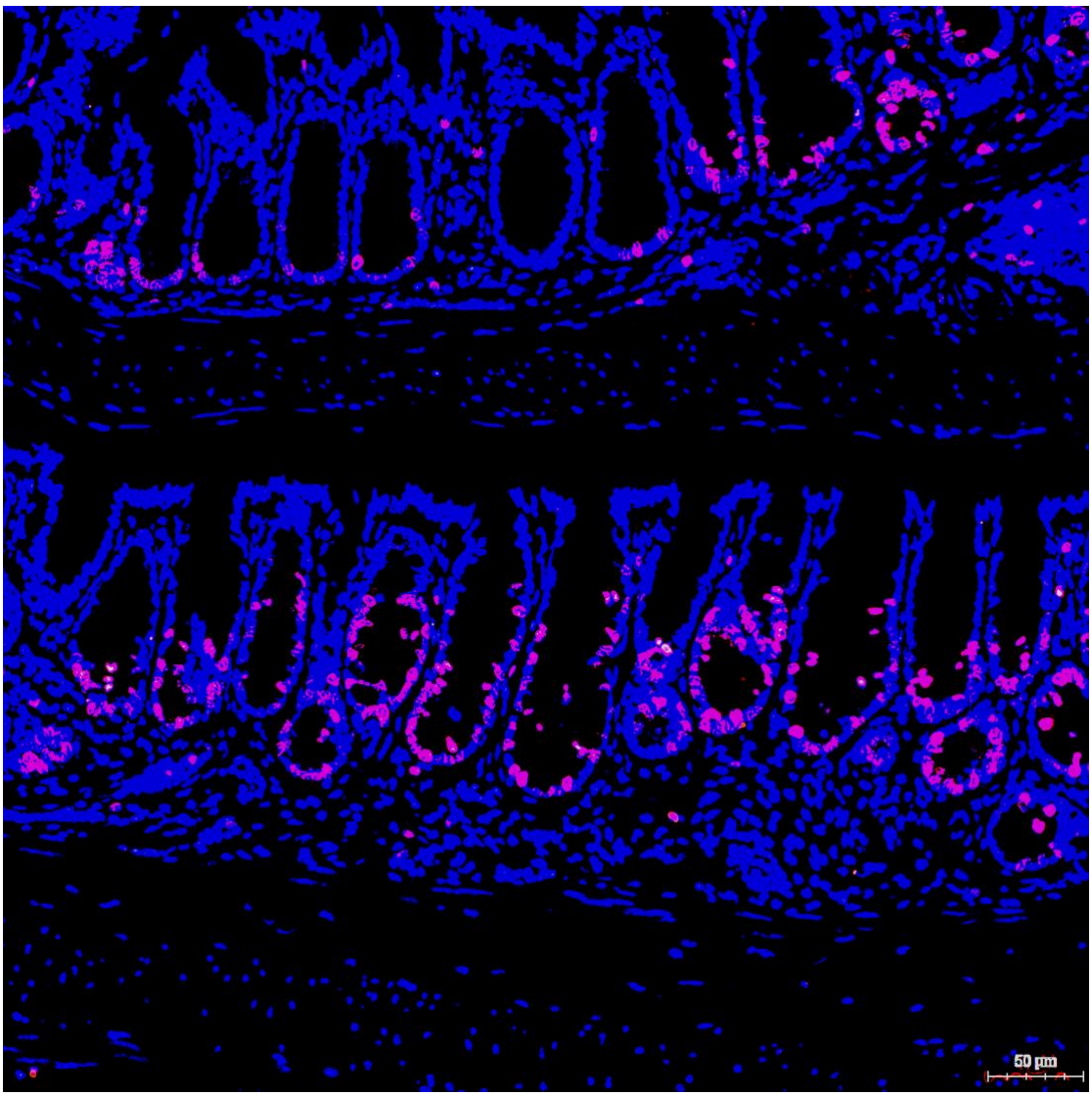

19. Figure: IF staining of KI67, scale bar = 50µm

The figure above (Figure 19) depicts an immunofluorescent staining of KI67 within colonic tissue. KI67 is a nuclear protein that is often used as a cellular proliferation marker. This enables the identification of the growth fraction in tissues and tumors. Figure 19 shows the crypts, small invaginations of intestinal tissue, the site of proliferation.[58,59]

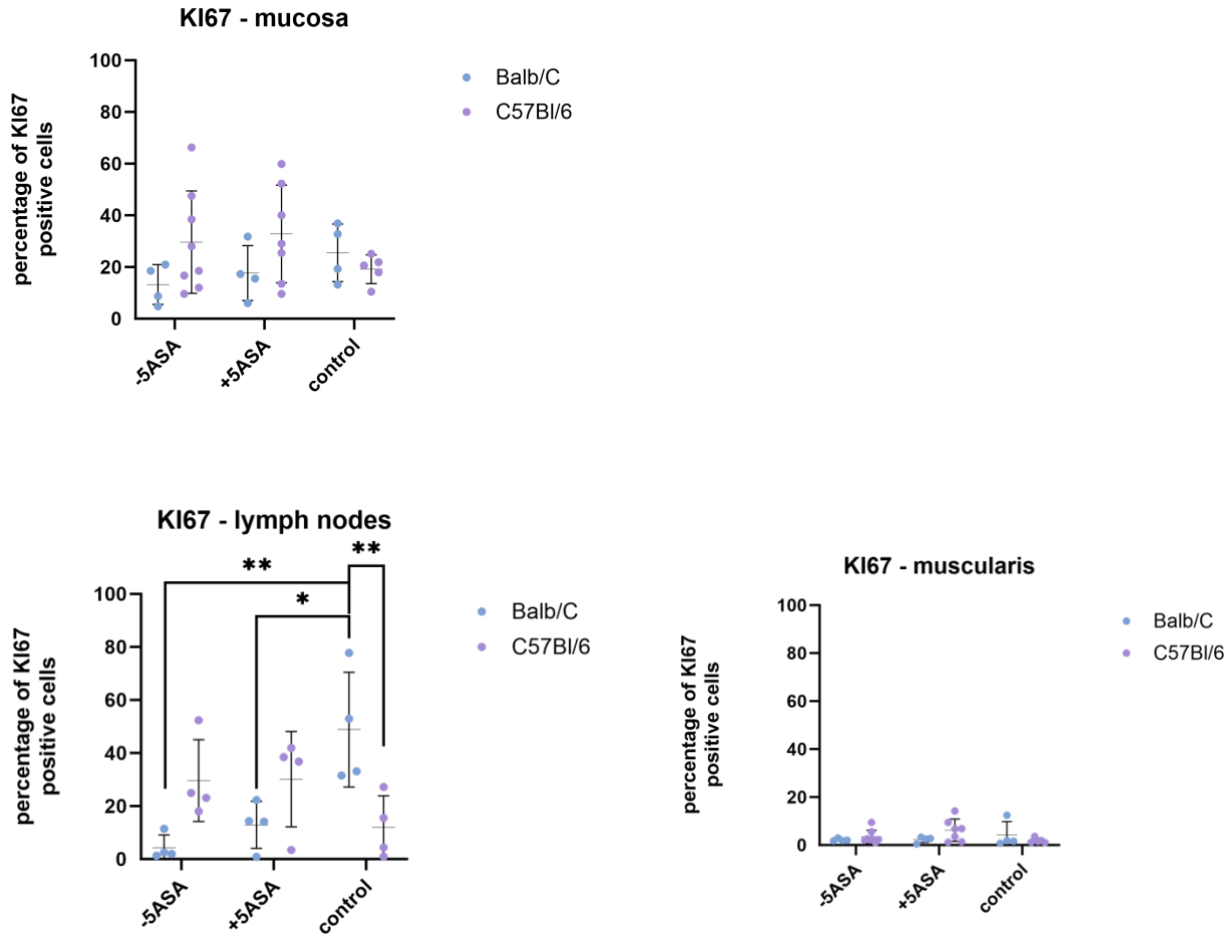

20. Figure: Percentages of KI67 positive cells of the mouse strains Balb/C and C57Bl/6 in the mucosa, muscularis and lymph nodes under different treatment conditions, with and without the anti-inflammatory treatment using 5-ASA. The percentage of KI67 positive cells are indicated on the y-axis, while the x-axis displays the treated, untreated and the control groups. The strain Balb/C is indicated in blue, and the C57Bl/6 is represented in purple.

In the mucosa, the percentage of KI67 positive cells increased after the 5-ASA treatment in both mouse strains. This effect was more pronounced in the C57Bl/6 mice. The control group, a healthy colonic tissue which did not receive any treatment, exhibited lower percentages of KI67 positive cells compared to the untreated mice.

The 20. Figure also shows that in the muscularis, the percentage of KI67 positive cells consistently remained the lowest for both mouse strains, regardless treatment. Only the C57Bl/6 mice showed a slight increase in their number of KI67 positive cells, still with no significant difference to the other groups.

In the lymph nodes, the 5-ASA treatment resulted in an elevation in the percentage of KI67 positive cells for Balb/C mice, but not for the C57Bl/6 mice. Although C57Bl/6 mice generally exhibited higher percentages of KI67 positive cells, this percentage did not increase following anti-inflammatory treatment. Interestingly, the control group of the Balb/C mice displayed the highest number of Ki67 positive cells in the lymph nodes, creating a significant difference between the treated and untreated group of the Balb/C mice. Similarly to the mucosa, the control group of the C57Bl/6 mice exhibited a lower percentage of positive KI67 cells compared to the other groups,

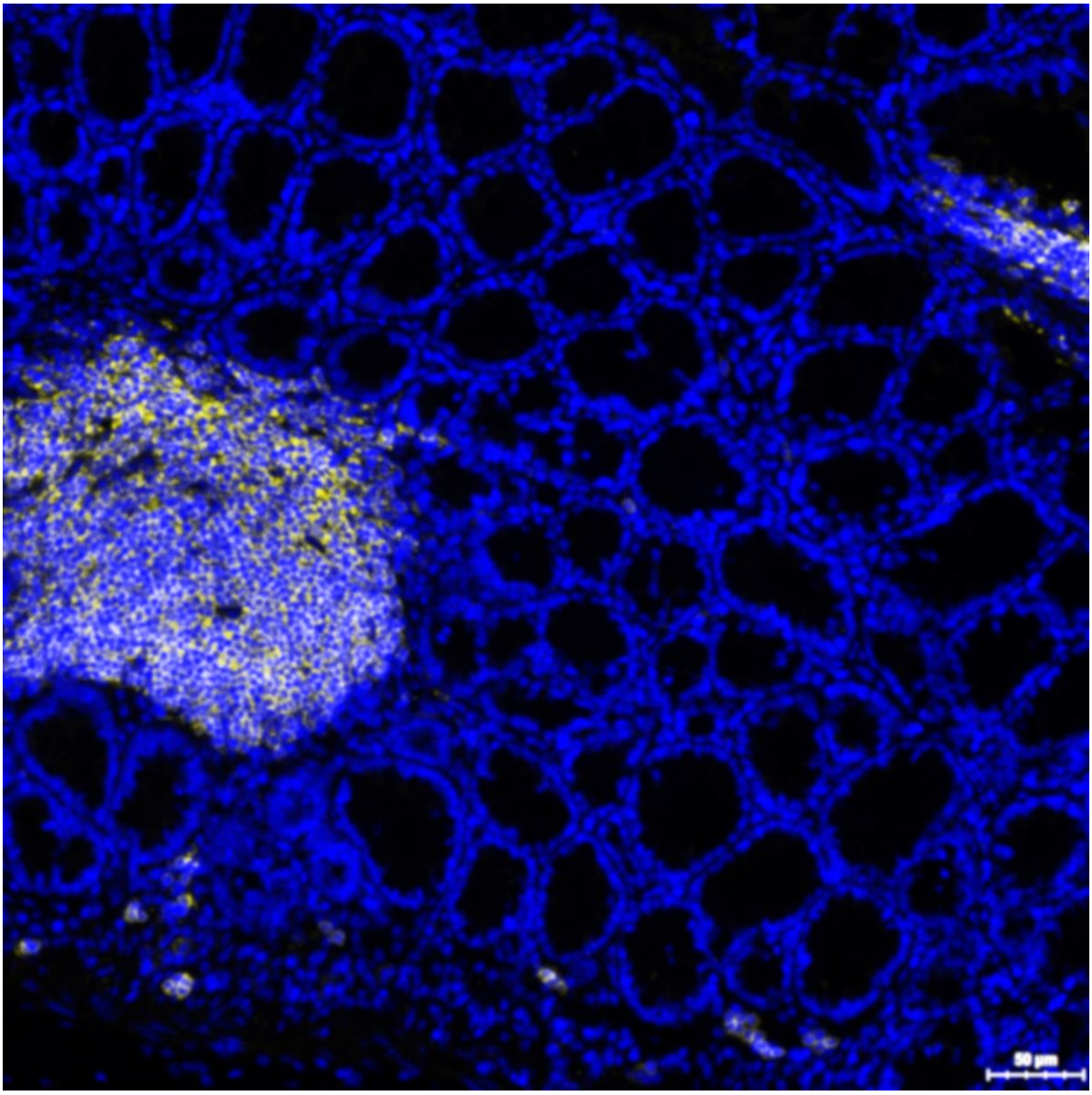

21. Figure: IF staining of CD20, scale bar = 50µm

The CD20 protein is a widespread B-cell marker expressed by most B cells[60]. The outcome of the staining, as depicted in Figure 21, indicates the success of the procedure, as the CD20 positive cells are predominantly located in the lymph nodes of the colonic tissue of the mice.

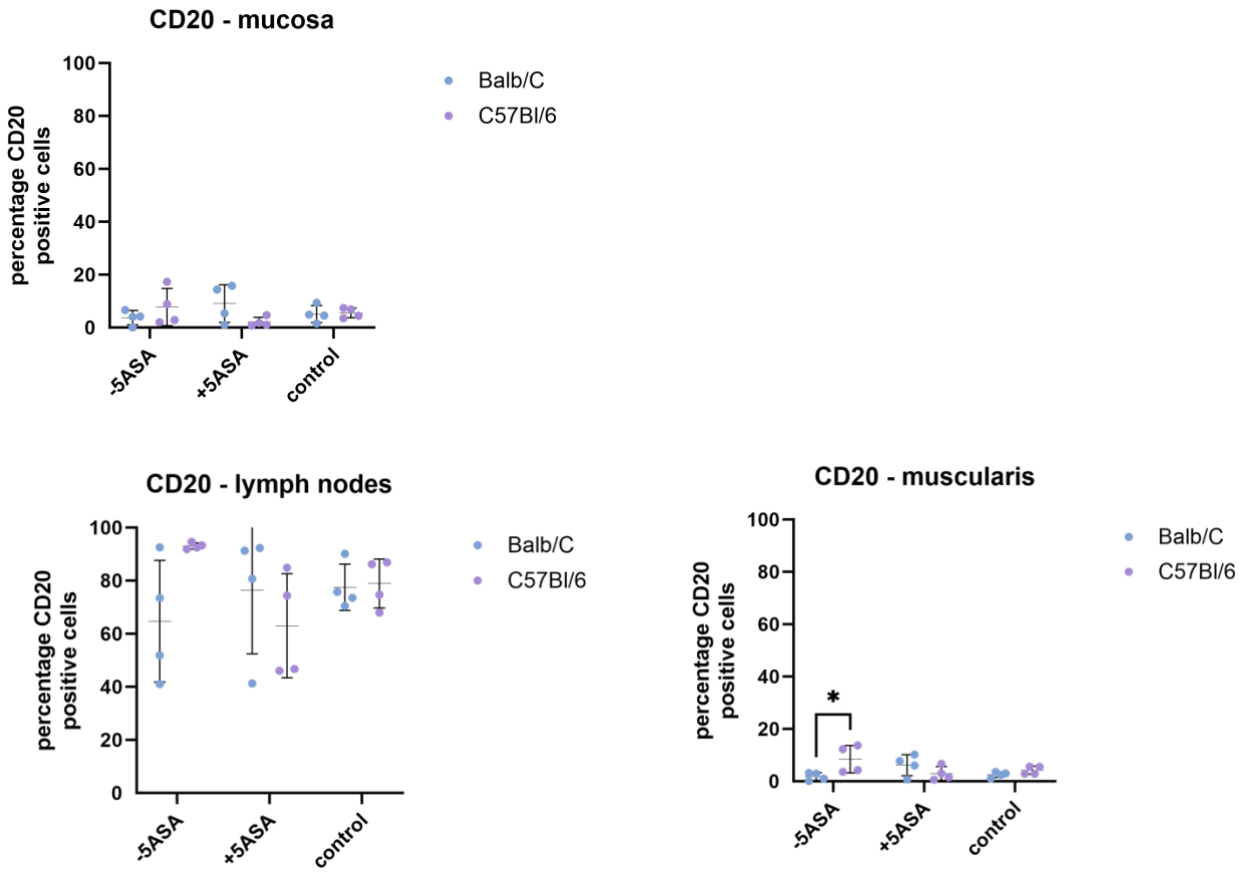

22. Figure: Percentages of CD20 positive cel cells of the mouse strains Balb/C and C57Bl/6 in the mucosa, muscularis and lymph nodes under different treatment conditions, with and without the anti-inflammatory treatment using 5-ASA. The percentage of CD20 positive cells are indicated on the y-axis, while the x-axis displays the treated, untreated and the control groups. The strain Balb/C is indicated in blue, and the strain C57Bl/6 is indicated in purple

As seen in the figure above, in the mucosa, the administration of 5-ASA treatment appeared to only have a minimal impact on the percentage of positive CD20 cells. Following treatment, Balb/C mice showed a slight increase, whereas C57Bl/6 mice exhibited a decrease. Control groups in both strains displayed low percentages of positive CD20 cells.

Lymph nodes exhibited the highest percentages of CD20 positive cells. While the anti-inflammatory treatment with 5-ASA led to a slight increase in the percentage of CD20 positive cells among the Balb/C mice, it had the opposite effect for the C57Bl/6 mouse strain, as they exhibited a 30% decrease in their percentage.

The control groups of the two mouse strains showed similar percentages for the CD20 positive cells. Notably, the control group of Balb/C mice had comparable CD20 positive cell levels,

while the control group of C57Bl/6 mice appeared to have more CD20 positive cells than the group treated with anti-inflammatory 5-ASA.

Discussion

In this study, my objective was to investigate the response of old mice to anti-inflammatory therapy using 5-ASA, and its impact on the development of colon cancer. It is noteworthy that colorectal cancer (CRC) is primarily a disease affecting older individuals, however, most research studies utilize young mice as models. By conducting this study, I aimed to bridge the gap between the experimental model and the target population, focusing on understanding how 5-ASA treatment influences colon cancer development in the context of aging.

I compared the expression levels of an inflammatory marker, an apoptotic marker, a marker of the Vitamin D system and of the Wnt pathway between the 18-month-old and 3-month-old mice.

By comparing the differences in the expression levels of these markers in this discussion, my aim was to provide a better understanding of the potential age-related differences in the therapeutic response to 5-ASA and its implications for colon cancer management in distinct age groups.

The inflammatory markers can indicate the presence or severity of inflammation in the body. Elevated levels of these markers can suggest the presence of inflammation. Changes in the levels of inflammatory markers can be used to evaluate the effectiveness of treatments for inflammatory conditions. If the treatment is working, there may be a decrease in the levels of these markers.[61]

The apoptotic markers, like the Bcl-2 family protein that were used in this project, can indicate the presence of apoptosis, which is programmed cell death. Apoptosis is a tightly regulated process that plays a crucial role in maintaining tissue homeostasis, eliminating damaged or unnecessary cells, and regulating cell populations during development. Changes in apoptotic marker levels or expression can be used to evaluate the effectiveness of treatments that induce or inhibit apoptosis. [62]

Markers of the Vitamin D system are substances or molecules that are associated with the metabolism, activation, and function of Vitamin D in the body. Vitamin D plays a crucial role

in calcium homeostasis, bone health, immune function, and many other physiological processes. The Vitamin D system involves several components, including its synthesis, transport, activation, and receptor-mediated effects. Some studies suggest that Vitamin D may have anti-cancer effects,[63,64] including in colorectal cancer. In the context of CAC, Vitamin D's anti-inflammatory and anti-proliferative effects may help in reducing the risk or progression of colorectal cancer associated with colitis.[65]

Markers of the Wnt pathway are associated with the activity, regulation, or components of the Wnt signaling pathway, which is a highly conserved signaling pathway that plays crucial roles in various biological processes, including cell proliferation, differentiation, migration, and survival. Dysregulation of the Wnt pathway has been implicated in many diseases, including cancer. Dysregulated Wnt signaling can promote tumor growth, invasion, and metastasis.[66]

The results showed a unique response to the treatment that differs depending on age, genetic strain of the mouse, and the specific segment of the colon under consideration. The treatment was most effective in the ascending colons of the young Balb/C mice while the older mice, regardless of their strain, exhibited minimal to no response to the treatment, irrespective of the strain.

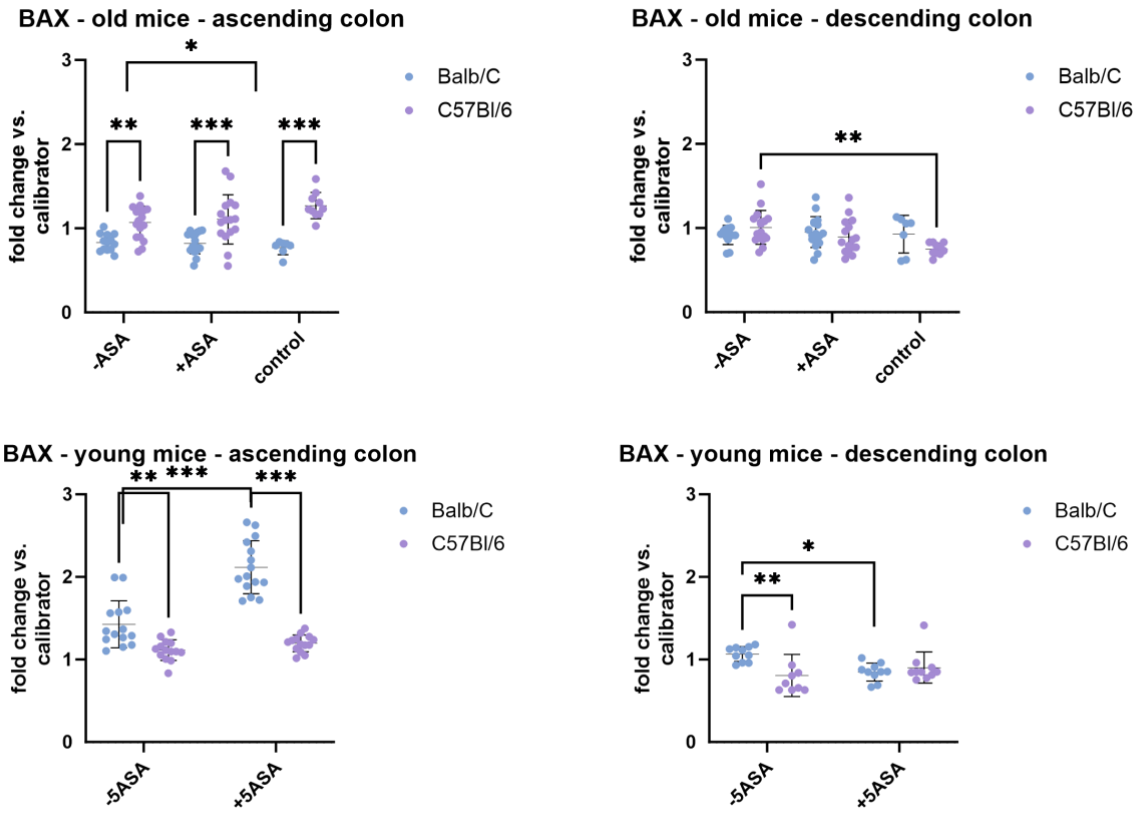

23. Figure: Expression levels for Bax in the ascending and descending colonic tissue of 3-month-old (referred to as "young") and 18-month-old (referred to as "old") mice. The lines between the dots indicate the mean. Values depicted on the y-axis indicate fold change expression vs. calibrator. The values on the x-axis represent the treatments, with "-5ASA" standing for the AOM/DSS treatment and "+5ASA" referring to the anti-inflammatory treatment with mesalazine that was administered to the mice after the AOM/DSS treatment. The "control" group did not receive any treatment and serves as a comparison to a healthy colon. Following a PCR, a two-way ANOVA (analysis of variance) was executed. Significantly distinct differences between groups are indicated by the presence of asterisks ($p<0.05$)

I compared the expression rates of PCR targets between 18-month-old and 3-month-old mice, using data from Nadja Kupper, a former PhD student in the Kallay lab, to illustrate the varying response to anti-inflammatory treatment with 5-ASA. Notably, the graphs for these age groups differ on the x-axis. The 3-month-old mice lack the control groups, as by the time of writing this thesis their data hasn´t been processed yet.

Interestingly, while young Balb/C mice displayed considerable changes in expression of the pro-apoptotic factor BAX following mesalazine treatment, older Balb/C mice exhibited a more moderate response, with modest upregulation in the ascending colon and slight

downregulation in the descending colon. For the C57Bl/6 mice, the anti-inflammatory treatment didn't provoke a strong response in either the old or young mice.

Comparing gene expression of Bax in different age groups of mice highlighted significant differences in their response to anti-inflammatory treatment. While the young mice exhibited varying reactions in different colonic tissues, the older mice, particularly in the Balb/C strain, showed less pronounced responses. This suggests a potential age-related variation in the efficacy of anti-inflammatory treatments, particularly noteworthy in different mouse strains.

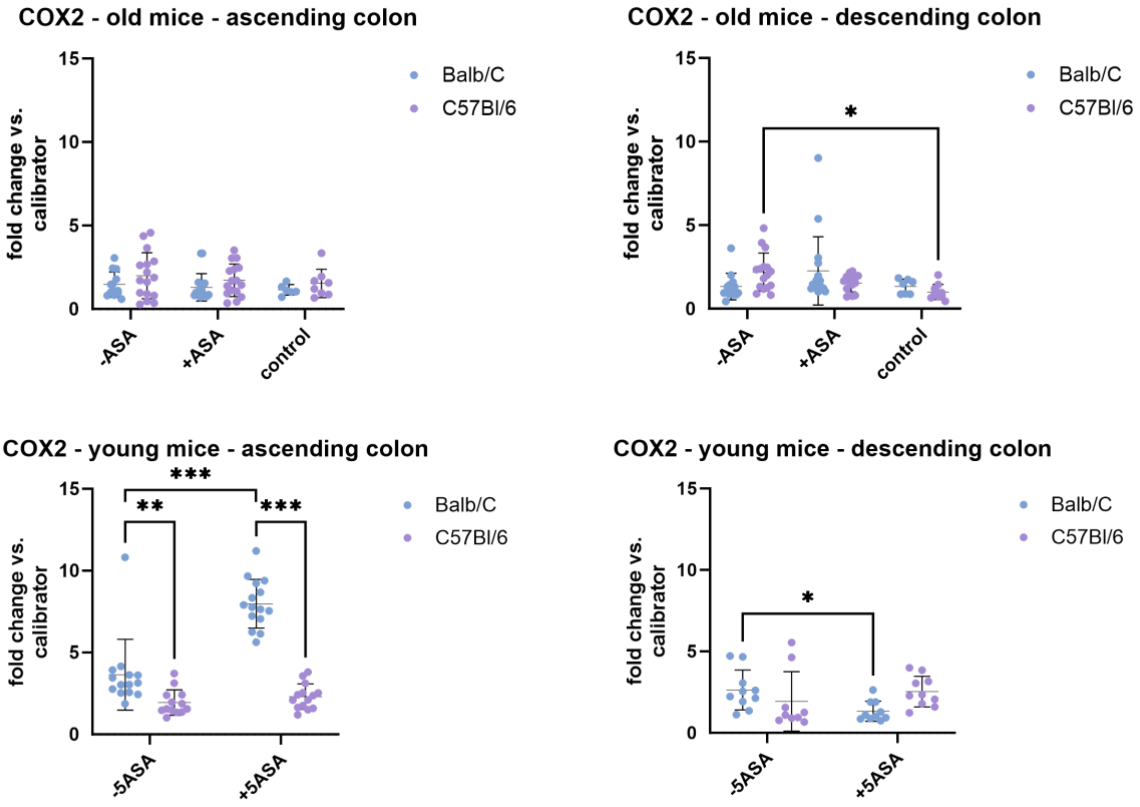

24. Figure: Figure: Expression levels for Cox2 in the ascending and descending colonic tissue of 3-month-old (referred to as "young") and 18-month-old (referred to as "old") mice. The lines between the dots indicate the mean. Values depicted on the y-axis indicate fold change expression vs. calibrator. The values on the x-axis represent the treatments, with "-5ASA" standing for the AOM/DSS treatment and "+5ASA" referring to the anti-inflammatory treatment with mesalazine that was administered to the mice after the AOM/DSS treatment. The "control" group did not receive any treatment and serves as a comparison to a healthy colon. Following a PCR, a two-way ANOVA (analysis of variance) was executed. Significantly distinct differences between groups are indicated by the presence of asterisks (p<0.05)

The observed differences in Cox2 expression following 5-ASA treatment highlight distinct responses between young Balb/C and C57Bl/6 mice and a lack of response in older mice.

These findings show that younger mice respond differently to anti-inflammatory treatment compared to older ones, especially in the way Cox2 behaves. Also, there are differences in Cox2 levels between different mouse strains and in tumors, indicating that how Cox2 works and reacts to treatment in colorectal tissues might vary depending on the strain of mice and the presence of tumors.

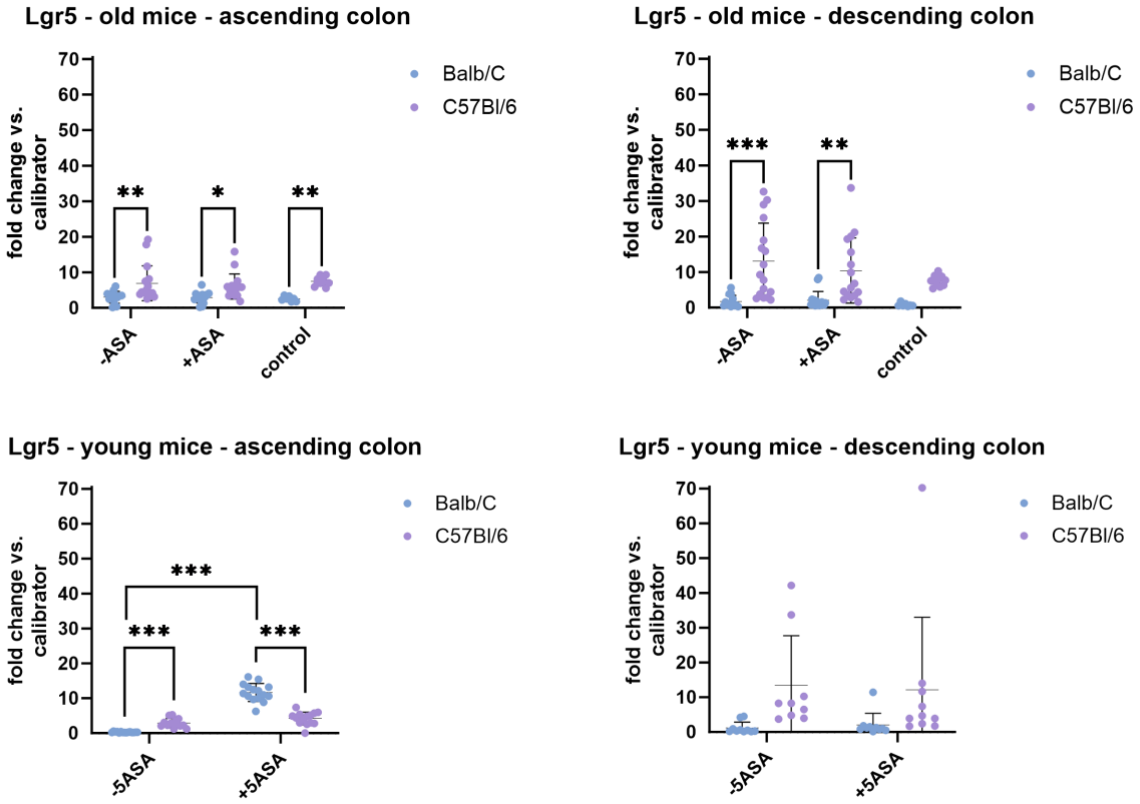

25. Figure: Expression levels for Lgr-5 in the ascending and descending colonic tissue of 3-month-old (referred to as "young") and 18-month-old (referred to as "old") mice. The lines between the dots indicate the mean. Values depicted on the y-axis indicate fold change expression vs. calibrator. The values on the x-axis represent the treatments, with "-5ASA" standing for the AOM/DSS treatment and "+5ASA" referring to the anti-inflammatory treatment with mesalazine that was administered to the mice after the AOM/DSS treatment. The "control" group did not receive any treatment and serves as a comparison to a healthy colon. Following a PCR, a two-way ANOVA (analysis of variance) was executed. Significantly distinct differences between groups are indicated by the presence of asterisks ($p<0.05$)

These findings indicate that the impact of anti-inflammatory treatments and the reaction to disease induction differ notably among mouse strains and age groups. This variance affects Lgr5 expression in distinct parts of the colon in varying ways.

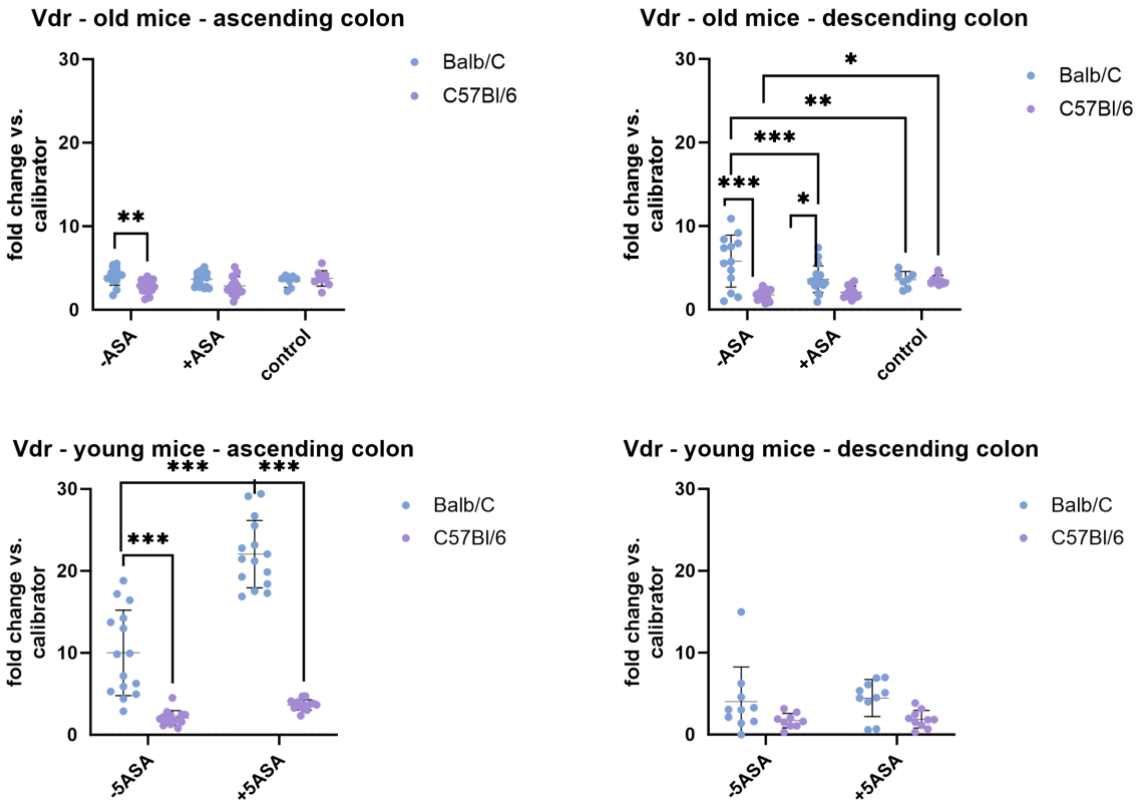

26. Figure: Expression levels for Vdr in the ascending and descending colonic tissue of 3-month-old (referred to as "young") and 18-month-old (referred to as "old") mice. The lines between the dots indicate the mean. Values depicted on the y-axis indicate fold change expression vs. calibrator. The values on the x-axis represent the treatments, with "-5ASA" standing for the AOM/DSS treatment and "+5ASA" referring to the anti-inflammatory treatment with mesalazine that was administered to the mice after the AOM/DSS treatment. The "control" group did not receive any treatment and serves as a comparison to a healthy colon. Following a PCR, a two-way ANOVA (analysis of variance) was executed. Significantly distinct differences between groups are indicated by the presence of asterisks ($p<0.05$)

These varied responses suggest that in the lower colon of older mice, there's a considerable impact of both disease induction and anti-inflammatory treatment on Vdr expression, with distinct patterns between mouse strains. Additionally, the notably low Vdr levels in the tumor groups across both strains indicate a potential association between tumor presence and reduced Vdr expression in this colon segment of older mice.

To further assess how the effect of the treatment on proliferation and immune infiltration differs in young and aged mice I compared the percentages of KI67 positive cells between 3-month-old and 18-month-old mice. While the data of the old mice is a product of my own work, the young mice were analyzed Sarah Guttman, a student in the Kallay lab.

Table 8 depicts the differences in KI67 positive cells of the mouse strains Balb/C and C57Bl/6 in the mucosa, muscularis and lymph nodes.

3. Table: Percentages of KI67 positive cells of the mouse strains Balb/C and C57Bl/6 in the mucosa, muscularis and lymph nodes of young and old mice. Table used with the approval of Sarah Guttman

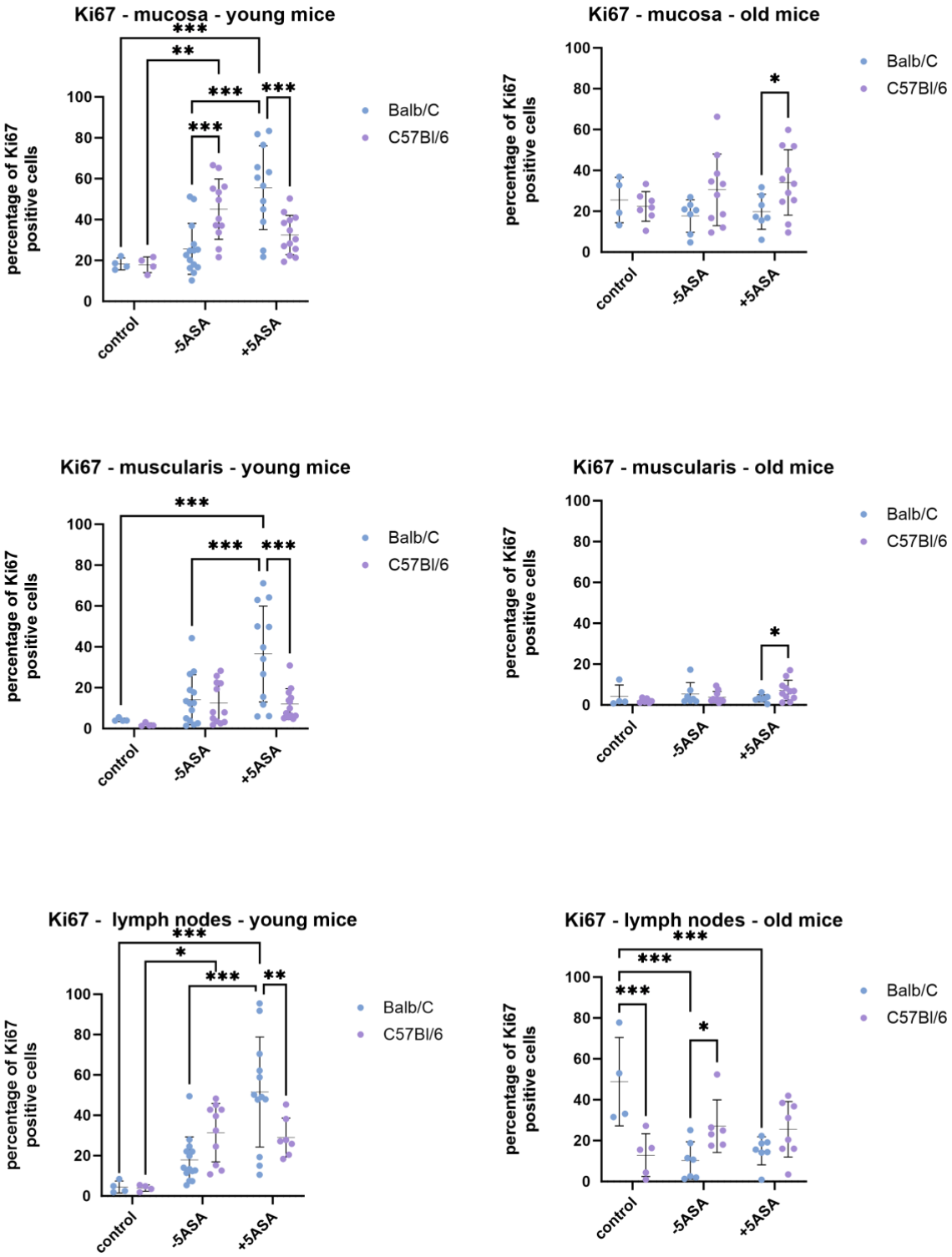

The percentage of KI67 positive cells are indicated on the y-axis, while the x-axis displays the treated, untreated and the control groups. The strain Balb/C is indicated in blue, and the C57Bl/6 is represented in purple. Notably, the graphs for these age groups differ on the x-

axis. The 3-month-old mice lack the control and tumor groups, as by the time of writing this thesis their data hasn´t been processed yet.
Young Balb/C mice show a notable rise in the portion of KI67 positive cells in the mucosa, muscularis, and lymph nodes following anti-inflammatory treatment when compared to older Balb/C mice. The older Balb/C mice had lower percentages of KI67 positive cells when treated with AOM/DSS, and this increased only slightly when given mesalazine.

In essence, the younger mice had more cells actively dividing in various parts of their bodies after anti-inflammatory treatment compared to the older mice. The older mice had fewer dividing cells when initially treated with AOM/DSS, and even with 5-ASA, the increase was minimal. This suggests that age affects the response to treatments targeting cell division in these mice.

In the older mice, the percentage of KI67 cells in the muscularis stayed consistently low and didn't show much variation regardless of the treatment used. However, among the young mice, there was a significant increase in the number of KI67 positive cells in the muscularis when they received anti-inflammatory treatment, but this effect was only seen in the Balb/C mice. Interestingly, the young C57Bl/6 mice didn't experience any change in the number of KI67 positive cells after being given mesalazine.

This indicates that the response to treatments affecting cell division differed between the age groups and mouse strains in the muscularis. Older mice showed consistent low cell division rates, while among the young mice, the response varied based on the type of treatment and mouse strain.

Among the older Balb/C mice, those that received AOM/DSS treatment had a notably lower percentage of KI67 positive cells in their lymph nodes compared to the control group, which had the highest number of these cells. Even after receiving 5-ASA treatment, there was hardly any increase in the number of KI67 cells.

On the other hand, in the young mice, mesalazine caused a significant increase in KI67 positive cells in the lymph nodes of Balb/C mice, but interestingly, the C57Bl/6 mice didn't seem to be affected by this treatment.

Essentially, the response to treatments in terms of cell division in the lymph nodes differed between older and younger mice, as well as between different strains of mice. Older mice showed reduced cell division rates, while the effects varied among the younger mice depending on the treatment and mouse strain.

4. Table: Percentages of CD20 positive cells of the mouse strains Balb/C and C57Bl/6 in the mucosa, muscularis and lymph nodes of young and old mice. Table used with the permission of Sahra Guttman.

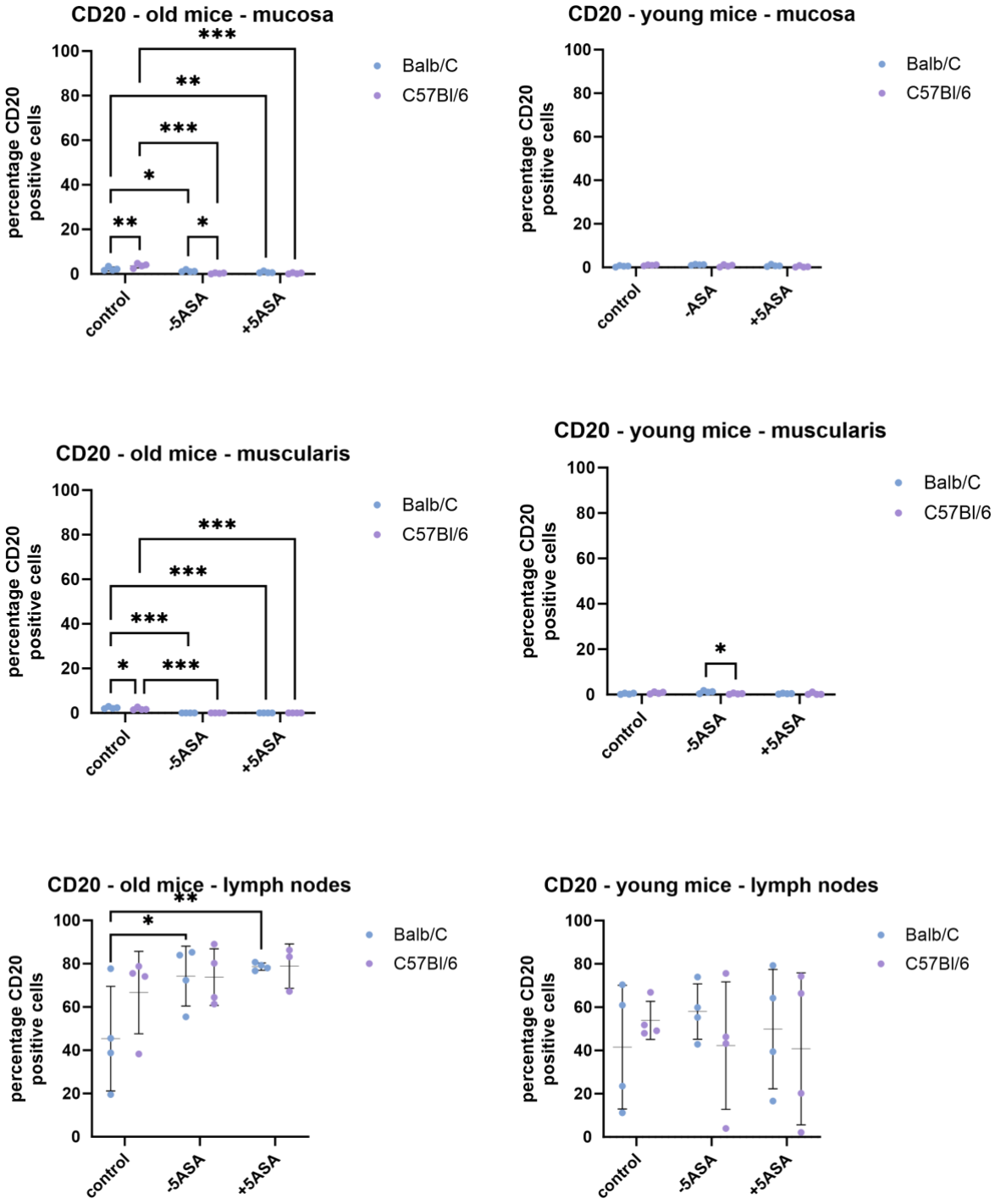

Furthermore, the analysis of the KI67 IF stainings provided a comparison between the Balb/C and C57Bl/6 mouse strains in their strain-specific responses.

In the mucosal tissue, the 5-ASA treatment is associated with a noticeable increase in the percentage of KI67 positive cells, which indicates an enhanced cell proliferation. This effect is particularly prominent in the C57Bl/6 mice, suggesting that this strain exhibits a stronger response to the treatment. Even the control group, which didn't receive any treatment, displayed slightly higher percentages of positive KI67 cells compared to the untreated mice. This could imply the presence of some intrinsic factors that influence cell proliferation in this context.

The findings regarding the muscularis reveal a consistent trend, as the percentage of KI67 positive cells remained consistently low in both mouse strains, irrespective of treatment status. This suggests that the muscularis may be less sensitive to the factors influencing cell proliferation, at least under the conditions of this study.

As for the lymph nodes, the effect of 5-ASA treatment is more nuanced. While there is a slight increase in the percentage of KI67 positive cells observed for Balb/C mice, the treatment appears to have little noticeable impact on the percentage of KI67 positive cells in the C57Bl/6 mice. This response shows potential variations in the effect of 5-ASA on cell proliferation in different tissue compartments.

Regarding the CD20 positive cells, in the mucosa, the impact of 5-ASA treatment on CD20-positive cells was minimal. Considering that CD20 is a B cell marker, the results are suggesting that this treatment might not significantly alter the B cell population within this tissue compartment. The slight increase in CD20-positive cells for Balb/C mice after treatment implies a potential response to the treatment, while the decrease in C57Bl/6 mice suggests a contrasting trend, possibly influenced by genetic factors or some specific immune responses.

Notably, a high percentage of CD20 positive cells was observed in the lymph nodes, suggesting a substantial presence of B cells in this tissue compartment. Following the anti-inflammatory treatment with 5-ASA, there was a slight increase in the percentage of CD20 positive cells for Balb/C mice, which points to a potential enhancement of B cell presence in the lymph nodes as a response to the treatment.

My work was not the first that researched the effect of AOM/DSS induced CAC in mice. A recent study of the Kallay group[67] also set out to examine CAC induction on mice in order to

gain a better understanding of the reaction to anti-inflammatory treatment. The Kallay group used 14-month-old Balb/C an C57Bl/6 mice which underwent CAC induction using the AOM/DSS model. The groups goals were to test if it's possible to induce CAC in older mice (older than 14 months, which roughly corresponds to 70-75 human years) to better resemble the human disease, and to test if it was possible to support tumor progression with low-level inflammation (1%DSS). Upon evaluating the results, the group stated that the 2.5% DSS was the best for comparing CAC in mice, (since he 3%DSS was too severe in Balb/C mice).

It has been shown before that mouse strains react differently to AOM/DSS treatment. Suzuki et al. [68] already evaluated the development of colon tumors in four different strains of mice: Balb/C, C3H/HeN, C57BL/6N and DBA/2N. Among the Balb/C mice, all showed colon adenocarcinoma, while 50% of the C57BL/6N mice had this condition. No tumors were detected in the other two strains of mice.
The experiment suggests that the combination of AOM and DSS caused colon adenocarcinoma in certain mouse strains, highlighting strain-specific susceptibilities, or responses to these compounds.

The differences in the reaction to CAC induction and in the reaction to the anti-inflammatory treatment between strains is great.
Because they are inbred, homozygous, and genetically stable, the Balb/C and C57Bl/6 mouse strains exhibit some disparities in their colonic structure and genetic composition that might impact how they respond to treatments involving mesalazine or AOM/DSS. Prior research has demonstrated behavioral shifts in mice, even within a genetically stable context, but whether these changes also reflect alterations in their genetic makeup and consequently affect their response to treatment remains uncertain. [69]

After analyzing the outcomes, I observed that the reaction to the treatment is mostly affected by their genetic strain. In both age groups the Balb/C strain showed the most sensitivity and response to the 5-ASA treatment, displaying significant alterations in the expression of target genes after receiving treatment. Conversely, the mice from the C57Bl/6 strain demonstrated considerably lower sensitivity, with their gene expression levels mostly unaffected by the

treatment. This implies that the anti-inflammatory therapy using 5-ASA had minimal to no impact on the C57Bl/6 strain.

These findings showcase the importance of considering the genetic background of the mice when evaluating the effectiveness of 5-ASA as an anti-inflammatory therapy, as the response can vary significantly between different mouse strains.

The findings from the study clearly indicate that the response to mesalazine (5-ASA) treatment is dependent on both age and mouse strain. Specifically, the expression levels of the target genes showed significant changes in the young Balb/C mice, suggesting a robust response to the anti-inflammatory treatment with 5-ASA. This strain exhibited the highest level of reaction to the treatment of the two mouse strains tested. These observations highlight the importance of considering both age and genetic background in evaluating the efficacy of 5-ASA as an anti-inflammatory therapy. They also underscore the potential of targeting specific subpopulations for optimized treatment outcomes.

Additionally, to the strain-differences, significant differences were observed in the response to the treatment between the ascending and descending colons. The ascending colon exhibited higher sensitivity to 5-ASA treatment compared to the descending colon. In the ascending part of the colon, the changes in expression levels of the target genes were more pronounced, indicating a stronger response to the treatment, while the differences in the descending colon were relatively less pronounced. These variations in sensitivity and response between the ascending and descending colons suggest that the effects of 5-ASA treatment may be influenced by the specific colonic segment, further adding complexity to the treatment response.

These results are consistent with findings from other studies, as the position of the tumor within the colon is increasingly seen as an important factor in assessing the progression of the disease, its prognosis, and treatment options.[70] Earlier research has shown that the main location of colon cancer can influence its development and molecular features. [71] The ascending and descending part of the colon has a different microbiota composition[72] and the higher presence of harmful bacteria on the left side of the colon is likely a key factor behind the increased occurrence of colon cancers affecting the descending colon.

While there is a common background in tumorigenesis in the ascending and descending colonic segments, like dysregulation of WNT/β-catenin pathway genes which affect the proliferative potential of CRC[73], the control of tumorigenesis has been shown to be side specific. [74]

Interestingly, the 5-ASA treatment didn't really affect the older mice, irrespective of their genetic strain or the part of their colon studied. Both the older Balb/C and C57Bl/6 mice showed very little change in their gene expression levels after receiving the 5-ASA treatment. This suggests that as mice age, this anti-inflammatory treatment might not work as effectively. Even with the treatment, the older mice didn't show big shifts in their gene expression, indicating that it might not have strong anti-inflammatory effects for them.

Given the significant difference in the reaction to anti-inflammatory treatment with 5-ASA between old and young mice, it is indeed more meaningful to consider conducting future experiments on older mice. The observed age-related variation in treatment response raises important questions about the underlying factors contributing to this disparity.

One possible explanation for the differing reactions could be the thinning of the mucus layer with age. As the mucus layer thins over time, it might make the older mice less susceptible to the anti-inflammatory effects of 5-ASA. In contrast, young mice with a healthier mucus layer may be less prone to developing colitis and subsequent colorectal cancer, making them more responsive to treatment.

This finding highlights the importance of investigating age-related changes in the colonic microenvironment, such as the mucosa, to gain a better understanding on the intricate interactions between aging, inflammation, and therapeutic responses. Such insights can guide the development of targeted and effective treatment strategies for age-related colonic disorders and hold implications for potential preventive measures.

However, there are certain questions that remain to be answered. Firstly, while the AOM/DSS model is widely used because of its high reproducibility, inexpensiveness, and user-friendliness, it is not standardized. The doses and duration of AOM and DSS exposure vary a

lot in different studies, which makes it tough to analyze and compare the experimental results.

Another limitation of this model deserves attention: there are significant differences in how colorectal cancer spreads invasively and metastasizes between animal models and the actual human disease. When diagnosed, approximately 50% of colorectal cancer patients exhibit lymphatic metastases and 33% show hematogenous metastases However, the occurrence of metastases is notably rare in AOM models of colorectal cancer. [75]

In human colorectal cancer, the disease typically advances in stages, often spreading through the bloodstream to the liver before reaching the lungs. However, liver metastases, which are common in human cases, are infrequent in rodent models of colorectal cancer induced by AOM. A recent study by Tanimura et al. showed that compared to AOM/DSS mice at 10 and 20 weeks, there was a notable increase in tumor infiltration into the submucosa and invasion into vessels at 30 weeks. This suggests that a longer duration of the experiment is necessary to better replicate the progression seen in human colorectal cancer. [76]

This study highlights the need to tailor treatment plans based on the mouse strain and research objectives in future studies using the AOM/DSS model[77]. While animal models of chemically induced colorectal cancers have offered valuable insights into human disease, many research avenues remain unexplored. Further investigations are essential to develop animal models that accurately replicate the process of metastasis.

Furthermore, it would be interesting to do the beforementioned tests on male mice. As CRC mainly affects the male population, it would be interesting to see if there are any sex-based differences to AOM/DSS treatment or to mesalazine between sexes.

List of Figures and Tables

Bibliography

(1) Baidoun F, Elshiwy K, Elkeraie Y, Merjaneh Z, Khoudari G, Sarmini MT, Gad M, Al-Husseini M, Saad A. Colorectal Cancer Epidemiology: Recent Trends and Impact on Outcomes. Curr Drug Targets. 2021;22(9):998-1009. Doi: 10.2174/1389450121999201117115717. PMID: 33208072.

(2) What Is Colorectal Cancer?, 2020. https://www.cancer.org/cancer/types/colon-rectal-cancer/about/what-is-colorectal-cancer.html (accessed 2023-07-25).

(3) Nagtegaal, I. D.; Quirke, P.; Schmoll, H.-J. Has the New TNM Classification for Colorectal Cancer Improved Care? *Nat. Rev. Clin. Oncol.* 2012, *9* (2), 119–123. https://doi.org/10.1038/nrclinonc.2011.157.

(4) Keum, N.; Giovannucci, E. Global Burden of Colorectal Cancer: Emerging Trends, Risk Factors and Prevention Strategies. *Nat. Rev. Gastroenterol. Hepatol.* 2019, *16* (12), 713–732. https://doi.org/10.1038/s41575-019-0189-8.

(5) Balchen, V.; Simon, K. Colorectal Cancer Development and Advances in Screening. *Clin. Interv. Aging* 2016, *Volume 11*, 967–976. https://doi.org/10.2147/CIA.S109285.

(6) Daniels, L. K. Rapid In-Office and in-Vivo Desensitization of an Injection Phobia Utilizing Hypnosis. *Am. J. Clin. Hypn.* 1976, *18* (3), 200–203. https://doi.org/10.1080/00029157.1976.10403798.

(7) Colorectal Cancer Risk Factors, 2023. https://www.cancer.org/cancer/types/colon-rectal-cancer/causes-risks-prevention/risk-factors.html (accessed 2023-10-04).

(8) Smith, R. J.; Bryant, R. G. Metal Substitutions Incarbonic Anhydrase: A Halide Ion Probe Study. *Biochem. Biophys. Res. Commun.* 1975, *66* (4), 1281–1286. https://doi.org/10.1016/0006-291x(75)90498-2.

(9) Cox, V. L.; Saeed Bamashmos, A. A.; Foo, W. C.; Gupta, S.; Yedururi, S.; Garg, N.; Kang, H. C. Lynch Syndrome: Genomics Update and Imaging Review. *RadioGraphics* 2018, *38* (2), 483–499. https://doi.org/10.1148/rg.2018170075.

(10) Nguyen, L. H.; Goel, A.; Chung, D. C. Pathways of Colorectal Carcinogenesis. *Gastroenterology* 2020, *158* (2), 291–302. https://doi.org/10.1053/j.gastro.2019.08.059.

(11) Grady, W. M.; Carethers, J. M. Genomic and Epigenetic Instability in Colorectal Cancer Pathogenesis. *Gastroenterology* 2008, *135* (4), 1079–1099. https://doi.org/10.1053/j.gastro.2008.07.076.

(12) Vogelstein, B.; Papadopoulos, N.; Velculescu, V. E.; Zhou, S.; Diaz, L. A.; Kinzler, K. W. Cancer Genome Landscapes. *Science* 2013, *339* (6127), 1546–1558. https://doi.org/10.1126/science.1235122.

(13) Boland, C. R.; Goel, A. Microsatellite Instability in Colorectal Cancer. *Gastroenterology* 2010, *138* (6), 2073-2087.e3. https://doi.org/10.1053/j.gastro.2009.12.064.

(14) Arnold, C. A.; Montgomery, E.; Iacobuzio-Donahue, C. A. The Serrated Pathway of Neoplasia: New Insights into an Evolving Concept. *Diagn. Histopathol.* 2011, *17* (9), 367–375. https://doi.org/10.1016/j.mpdhp.2011.06.006.

(15) De Palma, F.; D'Argenio, V.; Pol, J.; Kroemer, G.; Maiuri, M.; Salvatore, F. The Molecular Hallmarks of the Serrated Pathway in Colorectal Cancer. *Cancers* 2019, *11* (7), 1017. https://doi.org/10.3390/cancers11071017.

(16) Nakamura, F.; Sato, Y.; Okamoto, K.; Fujino, Y.; Mitsui, Y.; Kagemoto, K.; Kawaguchi, T.; Miyamoto, H.; Muguruma, N.; Sonoda, T.; Tsuneyama, K.; Takayama, T. Colorectal Carcinoma Occurring via the Adenoma–Carcinoma Pathway in Patients with Serrated Polyposis Syndrome. *J. Gastroenterol.* 2022, *57* (4), 286–299. https://doi.org/10.1007/s00535-022-01858-8.

(17) Zhou, Y.-J.; Lu, X.-F.; Chen, H.; Wang, X.-Y.; Cheng, W.; Zhang, Q.-W.; Chen, J.-N.; Wang, X.-Y.; Jin, J.-Z.; Yan, F.-R.; Chen, H.; Li, X.-B. Single-Cell Transcriptomics Reveals Early Molecular and Immune Alterations Underlying the Serrated Neoplasia Pathway Toward Colorectal Cancer. *Cell. Mol. Gastroenterol. Hepatol.* 2023, *15* (2), 393–424. https://doi.org/10.1016/j.jcmgh.2022.10.001.

(18) d'Aldebert, E.; Quaranta, M.; Sébert, M.; Bonnet, D.; Kirzin, S.; Portier, G.; Duffas, J.-P.; Chabot, S.; Lluel, P.; Allart, S.; Ferrand, A.; Alric, L.; Racaud-Sultan, C.; Mas, E.; Deraison, C.; Vergnolle, N. Characterization of Human Colon Organoids From Inflammatory Bowel Disease Patients. *Front. Cell Dev. Biol.* 2020, *8*, 363. https://doi.org/10.3389/fcell.2020.00363.

(19) Panaccione, R.; Ferraz, J.; Beck, P. Advances in Medical Therapy of Inflammatory Bowel Disease. *Curr. Opin. Pharmacol.* 2005, S1471489205001578. https://doi.org/10.1016/j.coph.2005.08.003.

(20) Neurath, M. F. Current and Emerging Therapeutic Targets for IBD. *Nat. Rev. Gastroenterol. Hepatol.* 2017, *14* (5), 269–278. https://doi.org/10.1038/nrgastro.2016.208.

(21) Axelrad, J. E.; Lichtiger, S.; Yajnik, V. Inflammatory Bowel Disease and Cancer: The Role of Inflammation, Immunosuppression, and Cancer Treatment. *World J. Gastroenterol.* 2016, *22* (20), 4794. https://doi.org/10.3748/wjg.v22.i20.4794.

(22) Ullman, T. A.; Itzkowitz, S. H. Intestinal Inflammation and Cancer. *Gastroenterology* 2011, *140* (6), 1807-1816.e1. https://doi.org/10.1053/j.gastro.2011.01.057.

(23) Pedersen, N.; Duricova, D.; Elkjaer, M.; Gamborg, M.; Munkholm, P.; Jess, T. Risk of Extra-Intestinal Cancer in Inflammatory Bowel Disease: Meta-Analysis of Population-Based Cohort Studies. *Am. J. Gastroenterol.* 2010, *105* (7), 1480–1487. https://doi.org/10.1038/ajg.2009.760.

(24) Parang, B.; Barrett, C. W.; Williams, C. S. AOM/DSS Model of Colitis-Associated Cancer. In *Gastrointestinal Physiology and Diseases*; Ivanov, A. I., Ed.; Methods in Molecular Biology; Springer New York: New York, NY, 2016; Vol. 1422, pp 297–307. https://doi.org/10.1007/978-1-4939-3603-8_26.

(25) Chen, J.; Huang, X.-F. The Signal Pathways in Azoxymethane-Induced Colon Cancer and Preventive Implications. *Cancer Biol. Ther.* 2009, *8* (14), 1313–1317. https://doi.org/10.4161/cbt.8.14.8983.

(26) Tanaka, T.; Kohno, H.; Suzuki, R.; Yamada, Y.; Sugie, S.; Mori, H. A Novel Inflammation-Related Mouse Colon Carcinogenesis Model Induced by Azoxymethane and Dextran Sodium Sulfate. *Cancer Sci.* 2003, *94* (11), 965–973. https://doi.org/10.1111/j.1349-7006.2003.tb01386.x.

(27) Mekler, L. B. On the Problem of Oncogene of Tumour Viruses. *Acta Virol.* 1975, *19* (6), 501–508.

(28) Okayasu, I.; Hatakeyama, S.; Yamada, M.; Ohkusa, T.; Inagaki, Y.; Nakaya, R. A Novel Method in the Induction of Reliable Experimental Acute and Chronic Ulcerative Colitis in Mice. *Gastroenterology* 1990, *98* (3), 694–702. https://doi.org/10.1016/0016-5085(90)90290-H.

(29) Kitajima, S.; Takuma, S.; Morimoto, M. Changes in Colonic Mucosal Permeability in Mouse Colitis Induced with Dextran Sulfate Sodium. *Exp. Anim.* 1999, *48* (3), 137–143. https://doi.org/10.1538/expanim.48.137.

(30) Rose, W. A.; Sakamoto, K.; Leifer, C. A. Multifunctional Role of Dextran Sulfate Sodium for in Vivo Modeling of Intestinal Diseases. *BMC Immunol.* 2012, *13* (1), 41. https://doi.org/10.1186/1471-2172-13-41.

(31) Parang B, Barrett CW, Williams CS. AOM/DSS Model of Colitis-Associated Cancer. Methods Mol Biol. 2016;1422:297-307. Doi: 10.1007/978-1-4939-3603-8_26. PMID:

27246042; PMCID: PMC5035391.

(32) Whetstone, R. D.; Wittel, U. A.; Michels, N. M.; Gulizia, J. M.; Gold, B. Colon Carcinogenesis in Wild Type and Immune Compromised Mice after Treatment with Azoxymethane, and Azoxymethane with Dextran Sodium Sulfate. *Mol. Carcinog.* 2016, *55* (7), 1187–1195. https://doi.org/10.1002/mc.22361.

(33) Veloso, P. M.; Machado, R.; Nobre, C. Mesalazine and Inflammatory Bowel Disease – From Well-Established Therapies to Progress beyond the State of the Art. *Eur. J. Pharm. Biopharm.* 2021, *167*, 89–103. https://doi.org/10.1016/j.ejpb.2021.07.014.

(34) Kaiser, G. C.; Yan, F.; Polk, D. B. Mesalamine Blocks Tumor Necrosis Factor Growth Inhibition and Nuclear Factor κB Activation in Mouse Colonocytes. *Gastroenterology* 1999, *116* (3), 602–609. https://doi.org/10.1016/S0016-5085(99)70182-4.

(35) Rousseaux, C.; Lefebvre, B.; Dubuquoy, L.; Lefebvre, P.; Romano, O.; Auwerx, J.; Metzger, D.; Wahli, W.; Desvergne, B.; Naccari, G. C.; Chavatte, P.; Farce, A.; Bulois, P.; Cortot, A.; Colombel, J. F.; Desreumaux, P. Intestinal Antiinflammatory Effect of 5-Aminosalicylic Acid Is Dependent on Peroxisome Proliferator–Activated Receptor-γ. *J. Exp. Med.* 2005, *201* (8), 1205–1215. https://doi.org/10.1084/jem.20041948.

(36) Mahida, Y. R.; Lamming, C. E.; Gallagher, A.; Hawthorne, A. B.; Hawkey, C. J. 5-Aminosalicylic Acid Is a Potent Inhibitor of Interleukin 1 Beta Production in Organ Culture of Colonic Biopsy Specimens from Patients with Inflammatory Bowel Disease. *Gut* 1991, *32* (1), 50–54. https://doi.org/10.1136/gut.32.1.50.

(37) Desreumaux, P.; Ghosh, S. Review Article: Mode of Action and Delivery of 5-Aminosalicylic Acid – New Evidence. *Aliment. Pharmacol. Ther.* 2006, *24* (s1), 2–9. https://doi.org/10.1111/j.1365-2036.2006.03069.x.

(38) Benavides, F.; Rülicke, T.; Prins, J.-B.; Bussell, J.; Scavizzi, F.; Cinelli, P.; Herault, Y.; Wedekind, D. Genetic Quality Assurance and Genetic Monitoring of Laboratory Mice and

Rats: FELASA Working Group Report. *Lab. Anim.* 2020, *54* (2), 135–148. https://doi.org/10.1177/0023677219867719.

(39) Pal-Ghosh, S.; Tadvalkar, G.; Jurjus, R. A.; Zieske, J. D.; Stepp, M. A. BALB/c and C57BL6 Mouse Strains Vary in Their Ability to Heal Corneal Epithelial Debridement Wounds. *Exp. Eye Res.* 2008, *87* (5), 478–486. https://doi.org/10.1016/j.exer.2008.08.013.

(40) How to Choose the Right Mouse Models and Genetic Modification Method for Your Research, 2020. https://www.cyagen.com/us/en/community/technical-bulletin/c57bl6-and-balbc-mouse.html#:~:text=BALB%2Fc%20mice%20tend%20to,while%20C57BL%2F6%20is%20H2b. (accessed 2023-06-20).

(41) Baran, B.; Mert Ozupek, N.; Yerli Tetik, N.; Acar, E.; Bekcioglu, O.; Baskin, Y. Difference Between Left-Sided and Right-Sided Colorectal Cancer: A Focused Review of Literature. *Gastroenterol. Res.* 2018, *11* (4), 264–273. https://doi.org/10.14740/gr1062w.

(42) Gervaz, P.; Bucher, P.; Morel, P. Two Colons-two Cancers: Paradigm Shift and Clinical Implications. *J. Surg. Oncol.* 2004, *88* (4), 261–266. https://doi.org/10.1002/jso.20156.

(43) Mik, M.; Berut, M.; Dziki, L.; Trzcinski, R.; Dziki, A. Right- and Left-Sided Colon Cancer – Clinical and Pathological Differences of the Disease Entity in One Organ. *Arch. Med. Sci.* 2017, *1*, 157–162. https://doi.org/10.5114/aoms.2016.58596.

(44) Huyghe, J. R.; Harrison, T. A.; Bien, et.al. Genetic Architectures of Proximal and Distal Colorectal Cancer Are Partly Distinct. *Gut* 2021, *70* (7), 1325–1334. https://doi.org/10.1136/gutjnl-2020-321534.

(45) Bufill, J. A. Colorectal Cancer: Evidence for Distinct Genetic Categories Based on Proximal or Distal Tumor Location. *Ann. Intern. Med.* 1990, *113* (10), 779. https://doi.org/10.7326/0003-4819-113-10-779.

(46) Skinner, S. A.; O'Brien, P. E. The Microvascular Structure of the Normal Colon in Rats and Humans. *J. Surg. Res.* 1996, *61* (2), 482–490. https://doi.org/10.1006/jsre.1996.0151.

(47) Araki, K.; Furuya, Y.; Kobayashi, M.; Matsuura, K.; Ogata, T.; Isozaki, H. Comparison of Mucosal Microvasculature between the Proximal and Distal Human Colon. *J. Electron Microsc. (Tokyo)* 1996, *45* (3), 202–206. https://doi.org/10.1093/oxfordjournals.jmicro.a023433.

(48) Polna, I.; Aleksandrowicz, J. Effect of Adsorbents on IgM and IgG Measles Antibodies. *Acta Virol.* 1975, *19* (6), 449–456.

(49) Danquah, K. O.; Adjei, E.; Quayson, S.; Adankwah, E.; Gyamfi, D.; Sampene, P. P.; Dzikunu, G.; Mensah, P.; Lepkor, C. Mucin Expression Patterns in Histological Grades of Colonic Cancers in Ghanaian Population. *Pan Afr. Med. J.* 2017, *27*. https://doi.org/10.11604/pamj.2017.27.267.9793.

(50) Shamsuddin, A. M.; Phelps, P. C.; Trump, B. F. Human Large Intestinal Epithelium: Light Microscopy, Histochemistry, and Ultrastructure. *Hum. Pathol.* 1982, *13* (9), 790–803. https://doi.org/10.1016/S0046-8177(82)80075-0.

(51) Arai, T.; Kino, I. Morphometrical and Cell Kinetic Studies of Normal Human Colorectal Mucosa. *Pathol. Int.* 1989, *39* (11), 725–730. https://doi.org/10.1111/j.1440-1827.1989.tb02421.x.

(52) Liu, L. U.; Holt, P. R.; Krivosheyev, V.; Moss, S. F. Human Right and Left Colon Differ in Epithelial Cell Apoptosis and in Expression of Bak, a pro-Apoptotic Bcl-2 Homologue. *Gut* 1999, *45* (1), 45–50. https://doi.org/10.1136/gut.45.1.45.

(53) Johnson. Laboratory Mice and Rats, 2023. https://doi.org///dx.doi.org/10.13070/mm.en.2.113.

(54) Lin, J.; Redies, C. Histological Evidence: Housekeeping Genes Beta-Actin and GAPDH

Are of Limited Value for Normalization of Gene Expression. *Dev. Genes Evol.* 2012, *222* (6), 369–376. https://doi.org/10.1007/s00427-012-0420-x.

(55) Magaki, S.; Hojat, S. A.; Wei, B.; So, A.; Yong, W. H. An Introduction to the Performance of Immunohistochemistry. In *Biobanking*; Yong, W. H., Ed.; Methods in Molecular Biology; Springer New York: New York, NY, 2019; Vol. 1897, pp 289–298. https://doi.org/10.1007/978-1-4939-8935-5_25.

(56) Cregger, M.; Berger, A. J.; Rimm, D. L. Immunohistochemistry and Quantitative Analysis of Protein Expression. *Arch. Pathol. Lab. Med.* 2006, *130* (7), 1026–1030. https://doi.org/10.5858/2006-130-1026-IAQAOP.

(57) D'Amico, F.; Skarmoutsou, E.; Stivala, F. State of the Art in Antigen Retrieval for Immunohistochemistry. *J. Immunol. Methods* 2009, *341* (1–2), 1–18. https://doi.org/10.1016/j.jim.2008.11.007.

(58) Liu, Q.; Ran, D.; Wang, L.; Feng, J.; Deng, W.; Mei, D.; Peng, Y.; Du, C. Association between Ki67 Expression and Therapeutic Outcome in Colon Cancer. *Oncol. Lett.* 2023, *25* (6), 272. https://doi.org/10.3892/ol.2023.13858.

(59) Wang, Y.; Ahmad, A. A.; Shah, P. K.; Sims, C. E.; Magness, S. T.; Allbritton, N. L. Capture and 3D Culture of Colonic Crypts and Colonoids in a Microarray Platform. *Lab. Chip* 2013, *13* (23), 4625. https://doi.org/10.1039/c3lc50813g.

(60) Pavlasova, G.; Mraz, M. The Regulation and Function of CD20: An "Enigma" of B-Cell Biology and Targeted Therapy. *Haematologica* 2020, *105* (6), 1494–1506. https://doi.org/10.3324/haematol.2019.243543.

(61) Menzel, A.; Samouda, H.; Dohet, F.; Loap, S.; Ellulu, M. S.; Bohn, T. Common and Novel Markers for Measuring Inflammation and Oxidative Stress Ex Vivo in Research and Clinical Practice—Which to Use Regarding Disease Outcomes? *Antioxidants* 2021, *10* (3), 414. https://doi.org/10.3390/antiox10030414.

(62) Ward, T. H.; Cummings, J.; Dean, E.; Greystoke, A.; Hou, J. M.; Backen, A.; Ranson, M.; Dive, C. Biomarkers of Apoptosis. *Br. J. Cancer* 2008, *99* (6), 841–846. https://doi.org/10.1038/sj.bjc.6604519.

(63) Carlberg, C.; Muñoz, A. An Update on Vitamin D Signaling and Cancer. *Semin. Cancer Biol.* 2022, *79*, 217–230. https://doi.org/10.1016/j.semcancer.2020.05.018.

(64) Seraphin, G.; Rieger, S.; Hewison, M.; Capobianco, E.; Lisse, T. S. The Impact of Vitamin D on Cancer: A Mini Review. *J. Steroid Biochem. Mol. Biol.* 2023, *231*, 106308. https://doi.org/10.1016/j.jsbmb.2023.106308.

(65) Dirks, N. F.; Cavalier, E.; Heijboer, A. C. Vitamin D: Marker, Measurand & Measurement. *Endocr. Connect.* 2023, *12* (4), e220269. https://doi.org/10.1530/EC-22-0269.

(66) Nagy, Á.; Tompa, M.; Krabóth, Z.; Garzuly, F.; Marái, A.; Kálmán, B. Wnt Pathway Markers in Low-Grade and High-Grade Gliomas. *Ideggyógy. Szle.* 2021, *74* (9–10), 349–355. https://doi.org/10.18071/isz.74.0349.

(67) Schepelmann, M.; Kupper, N.; Gushchina, V.; Mesteri, I.; Manhardt, T.; Moritsch, S.; Müller, C.; Piatek, K.; Salzmann, M.; Vlasaty, A.; Eferl, R.; Kallay, E. AOM/DSS Induced Colitis-Associated Colorectal Cancer in 14-Month-Old Female Balb/C and C57/Bl6 Mice—A Pilot Study. *Int. J. Mol. Sci.* 2022, *23* (9), 5278. https://doi.org/10.3390/ijms23095278.

(68) Suzuki, R.; Kohno, H.; Sugie, S.; Nakagama, H.; Tanaka, T. Strain Differences in the Susceptibility to Azoxymethane and Dextran Sodium Sulfate-Induced Colon Carcinogenesis in Mice. *Carcinogenesis* 2005, *27* (1), 162–169. https://doi.org/10.1093/carcin/bgi205.

(69) Shoji, H.; Miyakawa, T. Age-related Behavioral Changes from Young to Old Age in Male Mice of a C57 BL /6J Strain Maintained under a Genetic Stability Program. *Neuropsychopharmacol. Rep.* 2019, *39* (2), 100–118. https://doi.org/10.1002/npr2.12052.

(70) The Cancer Genome Atlas Network. Comprehensive Molecular Characterization of

Human Colon and Rectal Cancer. *Nature* 2012, *487* (7407), 330–337. https://doi.org/10.1038/nature11252.

(71) Gao, X. H.; Yu, G. Y.; Gong, H. F.; Liu, L. J.; Xu, Y.; Hao, L. Q.; Liu, P.; Liu, Z. H.; Bai, C. G.; Zhang, W. Differences of Protein Expression Profiles, KRAS and BRAF Mutation, and Prognosis in Right-Sided Colon, Left-Sided Colon and Rectal Cancer. *Sci. Rep.* 2017, *7* (1), 7882. https://doi.org/10.1038/s41598-017-08413-z.

(72) Zhong, M.; Xiong, Y.; Ye, Z.; Zhao, J.; Zhong, L.; Liu, Y.; Zhu, Y.; Tian, L.; Qiu, X.; Hong, X. Microbial Community Profiling Distinguishes Left-Sided and Right-Sided Colon Cancer. *Front. Cell. Infect. Microbiol.* 2020, *10*, 498502. https://doi.org/10.3389/fcimb.2020.498502.

(73) De Robertis, M.; Arigoni, M.; Loiacono, L.; Riccardo, F.; Calogero, R. A.; Feodorova, Y.; Tashkova, D.; Belovejdov, V.; Sarafian, V.; Cavallo, F.; Signori, E. Novel Insights into Notum and Glypicans Regulation in Colorectal Cancer. *Oncotarget* 2015, *6* (38), 41237–41257. https://doi.org/10.18632/oncotarget.5652.

(74) Mukund, K.; Syulyukina, N.; Ramamoorthy, S.; Subramaniam, S. Right and Left-Sided Colon Cancers - Specificity of Molecular Mechanisms in Tumorigenesis and Progression. *BMC Cancer* 2020, *20* (1), 317. https://doi.org/10.1186/s12885-020-06784-7.

(75) Rosenberg, D. W.; Giardina, C.; Tanaka, T. Mouse Models for the Study of Colon Carcinogenesis. *Carcinogenesis* 2008, *30* (2), 183–196. https://doi.org/10.1093/carcin/bgn267.

(76) Tanimura, Y.; Fukui, T.; Horitani, S.; Matsumoto, Y.; Miyamoto, S.; Suzuki, R.; Tanaka, T.; Tomiyama, T.; Ikeura, T.; Ando, Y.; Nishio, A.; Okazaki, K. Long-term Model of Colitis-associated Colorectal Cancer Suggests Tumor Spread Mechanism and Nature of Cancer Stem Cells. *Oncol. Lett.* 2020, *21* (1), 1–1. https://doi.org/10.3892/ol.2020.12268.

(77) Arnesen, H.; Müller, M. H. B.; Aleksandersen, M.; Østby, G. C.; Carlsen, H.; Paulsen, J. E.; Boysen, P. Induction of Colorectal Carcinogenesis in the C57BL/6J and A/J Mouse Strains

with a Reduced DSS Dose in the AOM/DSS Model. *Lab. Anim. Res.* 2021, *37* (1), 19. https://doi.org/10.1186/s42826-021-00096-y.